Inversion of legacy airborne electromagnetic datasets to inform the hydrogeological understanding of the northern Eyre Peninsula, South Australia

Ley-Cooper AY, Munday T, Gilfedder M,
Ibrahimi T, Annetts D, and Cahill K

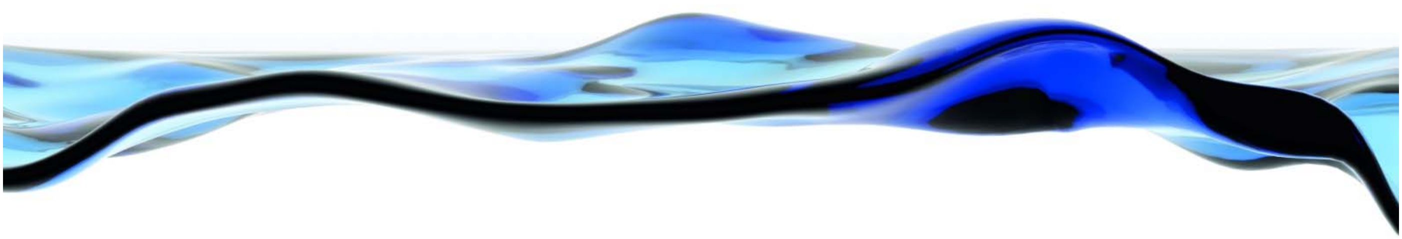

Goyder Institute for Water Research
Technical Report Series No. 15/50

GOYDER INSTITUTE FOR WATER RESEARCH

www.goyderinstitute.org

Goyder Institute for Water Research Technical Report Series ISSN: 1839-2725

The Goyder Institute for Water Research is a partnership between the South Australian Government through the Department of Environment, Water and Natural Resources, CSIRO, Flinders University, the University of Adelaide and the University of South Australia. The Institute will enhance the South Australian Government's capacity to develop and deliver science-based policy solutions in water management. It brings together the best scientists and researchers across Australia to provide expert and independent scientific advice to inform good government water policy and identify future threats and opportunities to water security.

The following Associate organisations contributed to this report:

Enquires should be addressed to: Goyder Institute for Water Research
Level 4, 33 King William Street
Adelaide, SA, 5000
tel: 08-8236 5200
e-mail: enquiries@goyderinstitute.org

Citation

Ley-Cooper AY, Munday T, Gilfedder M, Ibrahimi T, Annetts D, and Cahill K, 2015, *Inversion of legacy airborne electromagnetic datasets to inform the hydrogeological understanding of the northern Eyre Peninsula, South Australia,* Goyder Institute for Water Research Technical Report Series No. 15/50, Adelaide, South Australia.

Copyright

Disclaimer

Contents

Figures

Tables

Acknowledgments

We would like to acknowledge the support of the Goyder Institute for Water Research, CSIRO Land and Water, and CSIRO Mineral Resources, in helping resource this project.

We gratefully acknowledge the support of the South Australian Department of Water, Environment and Natural Resources (DEWNR), including Neil Power and Adrian Costar, and the South Australian Department of State Development (DSD), notably Miles Davies and Steve Hill for their support in acquiring additional AEM data for the project through PACE.

The Project would not have been successful without the generous support of the minerals industry and contractors, and we extend our thanks to Monax Mining, Spencer Resources, Adelaide Resources, Marmota Energy, Investigator Minerals, Cameco, UraniumSA and Geosolutions Pty Ltd.

Advice, input and feedback on the application of the Geoscience Australia LEI code was provided by Ross Brodie and we are very grateful for his time. Julian Vrbancich (DSTO) is also thanked for his advice on the calibration of REPTEM data.

Executive summary

For large-scale regional groundwater surveys, airborne electromagnetic (AEM) methods offer an efficient way of investigating the subsurface electrical conductivity (or its converse, the resistivity) and its spatial variability over large areas in a timely manner and at a relatively low cost (e.g. Siemon *et al.* 2009). Because electrical conductivity variability can be related to geological structure (good conductors such as metallic minerals containing iron or copper versus poor conductors including metamorphic rocks) and hydrogeological features (fresh versus saline groundwater), analysis of AEM data provides a means to determine stratigraphic boundaries and variations in groundwater salinity (Boulding 1993). Accurate processing and editing of AEM data is one of the crucial steps in obtaining quantitative geological information from these data sets which can then be used to underpin groundwater modelling and management.

This report describes several options for inverting 17 historical AEM datasets, which were originally acquired by exploration companies and government agencies at fine to regional scales. These surveys were used for minerals exploration, including graphite, palaeochannel uranium, silver, copper and base metals.

This report summarises the processing, inversion and analysis of these AEM datasets. Geophysical inversion aims to find models that explain geophysical observations; by using a model-based inversion method, one attempts to infer model parameters by iteratively fitting observations with theoretical predictions from trial models. Two inversion methods have been applied in this work:

- <u>Standard deterministic inversion</u> that looks for a single 'best' model through an iterative process using a so-called local optimization approach such as the gradient-based method. This work shows that deterministic inversions can accurately recover the broad type of geo-electrical structures, which are sought after when looking at regional hydrogeological features such as water bearing palaeochannels.
- <u>Bayesian analysis</u>, by using a Markov chain Monte Carlo Inversion (MCMC) algorithm on any of the AEM datasets of this work. This involves sampling thousands of varying plausible simulations, which provides probability distributions, rather than a single value, for the number of layers, thicknesses, depths and electrical conductivities values. MCMC is known as a global optimisation method, employing a global search approach to find the absolute minimum of an objective function so that predicted data best fit the observations (Everett 2013; Sen and Stoffa 2013). The MCMC analysis has revealed that that properly modelled deterministic inversions are usually a reasonable approximation of the whole suite of models recovered by the MCMC. One of the benefits of an MCMC inversion is the quantification of model uncertainty and what the main sources of uncertainty are. Further studies should be undertaken to investigate:
    1. how these uncertainties can be incorporated into hydrogeological modelling for groundwater resource determination, and,
    2. which of the geophysical uncertainties have the largest effect on hydrogeological uncertainties.

Modelling the whole suite of datasets has enabled us to transform legacy AEM data into maps and cross-sections that show the distribution of conductive (for EM signals) regolith material with depth. Results indicate conductive material is mapped in areas that can be associated with salt water intrusions, as well as where transported sediments are located (e.g. lacustrine clays and fluviatile sands in palaeovalleys). Mapping these conductors at varying depths gives an insight into distributions, volumes and extensions to potential aquifers and other sediment-filled features. To determine the materials which are responsible of the main conductive responses, results need to be validated with drilling and lithologic interpretation.

The project has demonstrated that AEM geophysical data can be inverted using MCMC analysis. MCMC analysis has several advantages over deterministic inversion, including the ability to derive a global optimum, the quantification of uncertainty around model outputs and correlations between model parameters. The project highlights the value of taking exploration geophysical datasets and applying them to extend our understanding of the hydrogeology of remote parts of South Australia.

We recommend that:

- Geological Survey of South Australia develop and maintain a directory of metadata relating to AEM systems and related surveys that details: date of acquisition, AEM system used, waveform employed, time gates used, and nominal system geometry.
- Derived models of subsurface conductivity from the inversion of AEM data sets should, in the absence of supporting drill-hole and ground data, be treated as providing a qualitative indication of groundwater quality and aquifer character. Where more detailed groundwater resource assessments are being undertaken in areas where AEM data are available, then work should be undertaken to validate derived conductivity models to inform groundwater model development as appropriate.
- Validation using results from targeted drilling be undertaken, including aquifer characterisation (petrophysical and hydraulic properties), borehole logging, aquifer testing, water sampling and analyses (tracers, Isotopes, and chemistry). A deficiency of both G-FLOWS Stage-1 and Stage-2 was the lack of available on-ground data to undertake detailed validation work, which can underpin the hydrogeological framework models that have been developed. Future projects should have a significant resource devoted to this.

1 Introduction

1.1 Background

Access to water is identified as a key infrastructure necessity for mining, energy and industry development, however, it is common knowledge that there is an inadequate level of knowledge of these resources and their capacity to meet the emerging industry demands. Water availability was identified as a challenge facing the development of mining in the “Research, Development and Innovation Roadmap for the South Australian Mining Industry” prepared for the South Australian Chamber of Mines and Energy (SACOME). The Infrastructure Demand Study undertaken in 2011 by the Resources and Energy Sector Infrastructure Council (RESIC) forecast that the annual water demand across the South Australian resource industry will increase from approximately 40 GL to over 170 GL per annum over the next 10 years. The scale of planned developments and potential activity from current mineral exploration is set to generate significant economic value for the State, but its realisation is dependent on access to groundwater resources. In South Australia, new mining and potential geothermal energy developments in the remote parts of South Australia (including northern Eyre Peninsula) is being facilitated by the South Australian Government through the Plan for Accelerated Exploration (PACE) Program coordinated by the Department of State Development.

The G-FLOWS Initiative of the Goyder Institute for Water Research linked to the South Australian Department of Water, Environment and Natural Resources (DEWNR) has been investigating whether minerals exploration data sets could be harnessed to expand our hydrogeological understanding of key areas in the State, namely, the northern Eyre Peninsula, the Musgrave Province and the Frome Embayment. These are considered as Tier 1 and Tier 2 areas for ongoing activities by the South Australian Government’s Department of State Development (DSD) and the Geological Survey of South Australia.

Information sought as part of this research includes the location, geometry and characteristics of key aquifers, their potential capacity and the quality and variability of the contained groundwater resources. Particular attention has been given to refining and applying methodologies and protocols, developed as part of G-FLOWS Stage-1 (Gilfedder and Munday 2013). These have been used to tie-in the information contained in airborne geophysical survey and other minerals exploration data with those from existing topographic and hydrogeological data suites. This provides a way to extend our understanding of groundwater resource potential in remote areas of the State. The research undertaken has also involved developing a spatial understanding of groundwater recharge and discharge processes and their rates (see Taylor *et al.* 2015).

High resolution airborne magnetics provide some insight into regolith thickness, although airborne electromagnetic (AEM) methods are perhaps the only cost effective technology for mapping spatial elements of the cover, aquifer and groundwater complexity at a broad-scale. The technology also provides constraints on the hydrogeology, and when linked with isotopic and tracer data, provides additional detail and understanding on the hydrogeological framework at fine scales (i.e. sub kilometre scale), which can benefit the analysis and interpretation of geochemical and hydrogeochemical data sets.

For large-scale regional groundwater surveys, airborne electromagnetic (AEM) methods offer an efficient way of investigating the geo-electrical structure over large areas in a timely manner and at relatively low cost (e.g. Siemon *et al.* 2009). However, accurate processing and editing of AEM data is one of the crucial steps in obtaining quantitative information from these data sets that can then be used for groundwater modelling and management (e.g. Christiansen *et al.* 2011, Viezzoli *et al.* 2013). When attempting to extract quantitative earth models from the AEM, the reliability of the model parameters fed into the inversion algorithm becomes crucial. An accurate inversion algorithm needs quality data, system noise information, precise forward modelling and reliable EM systems specifications in order to achieve usable outcomes.

These elements are not always available, particularly when dealing with legacy datasets. Therefore, a significant amount of effort was directed to securing this information in part of this project.

The general context in which inverted AEM models have been used in the G-FLOWS Stage-2 project, is by providing additional information on the spatial distribution, character, connectivity and groundwater quality of aquifer systems (saline versus fresh). This report describes the challenges of inverting historical AEM datasets that were originally acquired by exploration companies and Government agencies at fine to regional scales, and intended for use in minerals exploration.

This report has also focused on steps taken to produce reasonable forward modelling for the different AEM systems that have been used in the area. In some cases ancillary datasets (including flights over seawater) have been used to gain some additional control over the expected response. Synthetic examples have also been run, to show the effect of inaccurate parameter description such as the geometry of the waveform on the results.

Project outputs are intended to inform the accessibility and viability of the South Australia's groundwater resources that are suitable for mineral processing and energy supply. While the outputs from this report do not directly define the groundwater resource character or potential of the areas they cover, the work does provide a framework that could be employed in particular localities where warranted. More generally, the intention is affirm its intention of encouraging and securing development where appropriate, while enabling prudent decision making and policies regarding water allocation, accounting, and licensing, whilst ensuring the protection of environmental assets.

1.2 Aims of this report

The aims of this report are to:

- Show the distribution of the different exploration geophysical data sets acquired as part of the G-FLOWS Stage-2 Project, with particular emphasis on airborne electromagnetic data.
- Detail the AEM acquisition systems employed and their characteristics.
- Show that historical AEM data can be modelled appropriately when parameters such as system geometry, sampling-windows, wave-forms and other system attributes are specifically accounted for.
- Detail how their interpretation, through use of a common inversion approach, can benefit the regional understanding of the hydrogeology of the northern Eyre Peninsula.
- Apply a Bayesian style inversion to an example dataset, in order to better handle uncertainties in the definition of subsurface conductivity structure, and to compare it against standard deterministic methods.

1.3 Study area and AEM data types

The area defined for this study covers the northern Eyre Peninsula (Figure 1), extending over an area from a line running east to west around ~60 km south of the towns of Elliston and Cleve, up to the southern margins of the Gawler Range Volcanics, bounded in the north by a line just north of Ceduna (in the west), extending across to Port Augusta in the east.

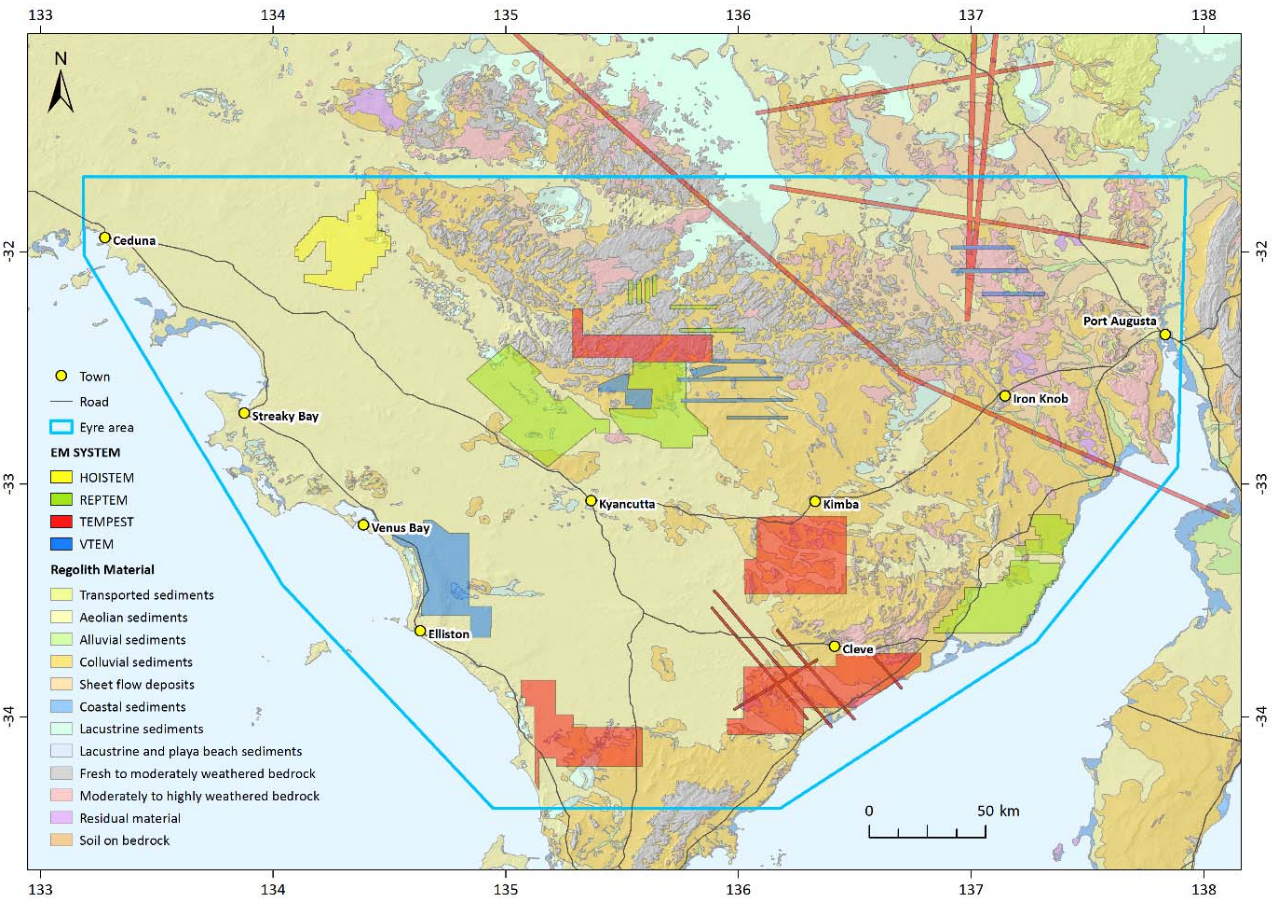

Figure 1 - A map of regolith materials covering the study area in the northern Eyre Peninsula in South Australia. The extent of the study area and the distribution of AEM data types is also defined. The survey areas and lines do not represent the complete coverage of airborne EM data across the Peninsula, but most of the coverage is shown. Although not studied here, several other smaller surveys and lines are known to exist in the area north of Cleve, over areas near Iron Knob, and to the north of Kimba.

Figure 1 also shows the spatial extent of the AEM datasets analysed as part of this project. Particulars of the different EM system types used are indicated by coloured lines or polygons. Most of these data were originally acquired for mineral exploration purposes. Work in the Goyder FLOWS Stage-1 Project (Gilfedder and Munday 2013) have shown that legacy airborne geophysical data can be reprocessed with the derived products used for mapping components of the hydrogeological system appropriate for near-surface groundwater investigations and resource assessments (e.g. Ley-Cooper and Munday 2013).

All airborne EM datasets analysed in the northern Eyre Peninsula study area were acquired by helicopter or fixed-wing time domain (TEM) systems. Data from four AEM systems (and variants) were analysed for the project. These comprised data from the HOISTEM, REPTEM and VTEM helicopter borne time domain AEM systems, and the TEMPEST fixed wing time domain AEM system. These are discussed in more detail in the following section, along with some background on the technique of AEM surveying.

2 Airborne Electromagnetic (AEM) systems used in the study area

2.1 The airborne electromagnetic (AEM) surveying technique

AEM surveying techniques involve the measurement of ground response to propagating electromagnetic (EM) fields. All time domain AEM systems consist of a transmitter (Tx) loop and a receiver coil (Rx), arranged in different geometries with associated electronics. Primary EM fields are generated by passing a large current through a loop or coil. The physics involved with a transient electromagnetic system is that when the current in the transmitter coil(s) is turned off quickly (in a few micro seconds), the change in the (primary) magnetic fields induces eddy (secondary) currents in the ground. A secondary EM field is induced in the ground and these fields are detected by the alternating currents that are induced to flow in a receiver coil, through a process known as electromagnetic induction (illustrated schematically in Figure 2). As the induction of current flow results from the magnetic component of the electromagnetic field, there is no need to have physical contact between the transmitter or receiver and the ground. Consequently, these surveys can proceed effectively on the ground or in the air.

In the presence of a conducting body (for example a conductive aquifer), the induced eddy or alternating currents flow in the conductor, generate the secondary electromagnetic field which decays over time and this is measured by the receiver (Peters 2001). The difference between the transmitted (primary) and received (secondary) electromagnetic fields is determined by the geometry and electrical properties of conductors in the ground. Materials that are highly conductive produce strong secondary electromagnetic fields and slow decay rates. Sedimentary materials such as those deposited in old buried valley systems (palaeovalleys), and porous saprolite can contain saline pore water which promotes the persistence of such fields. These materials are present in many parts of the northern Eyre Peninsula and are therefore deemed as good targets for the application of AEM surveying techniques.

2.2 Factors affecting ground conductivity

The influence of particular characteristics of aquifer sediments and the underlying basement lithologies on the observed geophysical response defined by an airborne electromagnetic system is summarised as follows. The electrical conductivity (the reciprocal of resistivity) of these materials is a measure of how easily an electrical current can pass through them. Conductivity itself is a complex function of a number of variables (Loke 2000) including:

- concentration of dissolved electrolytes - the concentration of ionic conductors in solution (e.g. saline water is more conductive than fresh water);
- amount (clayey sediments are more conductive than sandy sediments) and composition of clays - particularly those with a moderate to high cation exchange capacity (CEC);
- moisture content - the extent to which the pores are filled with water (EC increases with increasing moisture content (e.g. Rhoades et al. 1976));
- porosity (intergranular and fractures): shape and size of pores, number, size and shape of interconnecting passages; and
- temperature (EC increases with increasing temperature; for different solutions, the temperature correction is about 0.5-3%/°C).

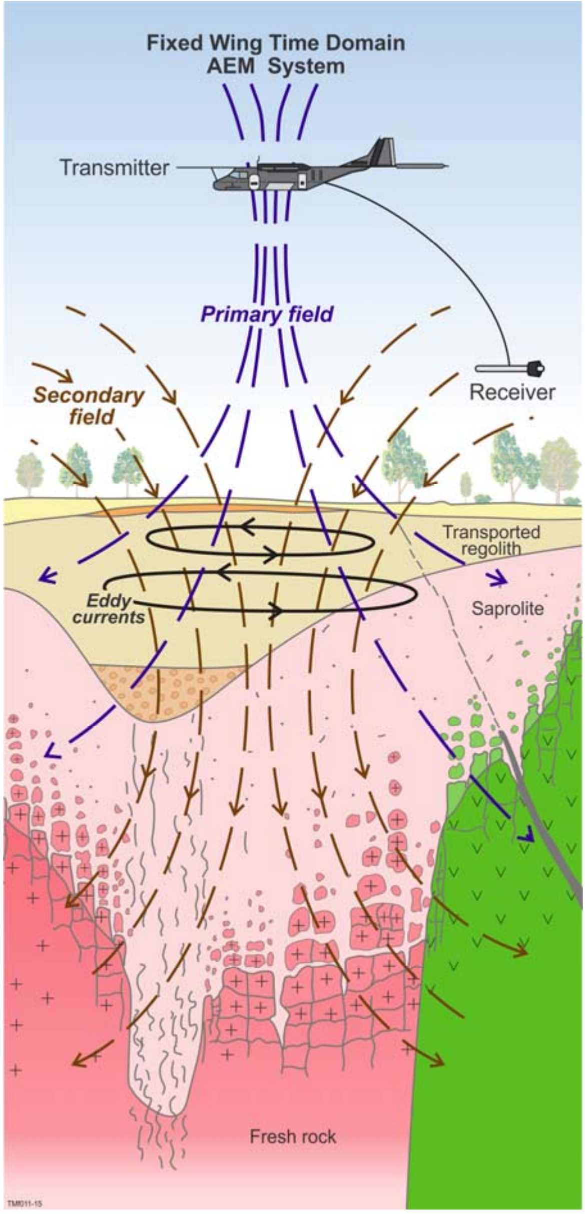

Figure 2 - Schematic diagram illustrating the operating principles involved in AEM data acquisition.

Sedimentary rocks, whether consolidated or unconsolidated are characterised by a range of conductivities (Figure 3), but the influence of contained water quality and quantity can also be significant (e.g. Palacky 1983). Generally speaking, it is reasonable to assume that the observed ground conductivity, whether measured by a ground or airborne system, would be non-unique for any given aquifer system. In both consolidated and unconsolidated regolith and sedimentary materials, including alluvial materials and underlying sedimentary or crystalline basement rocks, the conductivity will be significantly influenced by the electrolyte (salt) which occurs in moisture-filled pores within an insulating matrix (McNeill 1980, 1990). Whilst the porosity and connectivity of the pores in sediments and in-situ regolith materials play a part in driving conductivity, particularly in the absence of clays, it is the quantity and in particular the quality of the contained pore water (i.e. total dissolved solids) that is critical (Paine et al. 2003). Clay content and type become important when the concentration of ionic conductors (for, example, salts in solution) is low. Their significance becomes negligible at high ionic concentrations, particularly for clays of low to moderate CEC, such as kaolinite (Emerson and Yang 1997). Given the saline to brackish quality of the groundwater contained in many of the transported materials and in-situ regolith materials present across the northern Eyre Peninsula, it is reasonable to expect that the observed conductivity structure in the airborne EM data set will reflect variations in water quality associated with particular regolith/sedimentary packages, rather than factors linked to sedimentary texture (i.e. grain size, and orientation). Nonetheless, a relationship between sediment type and salinity may occur. Silts and clays may often contain more saline groundwater, since they are relatively impermeable, and groundwater moves slowly through them thus encouraging the accumulation of salts in their pores.

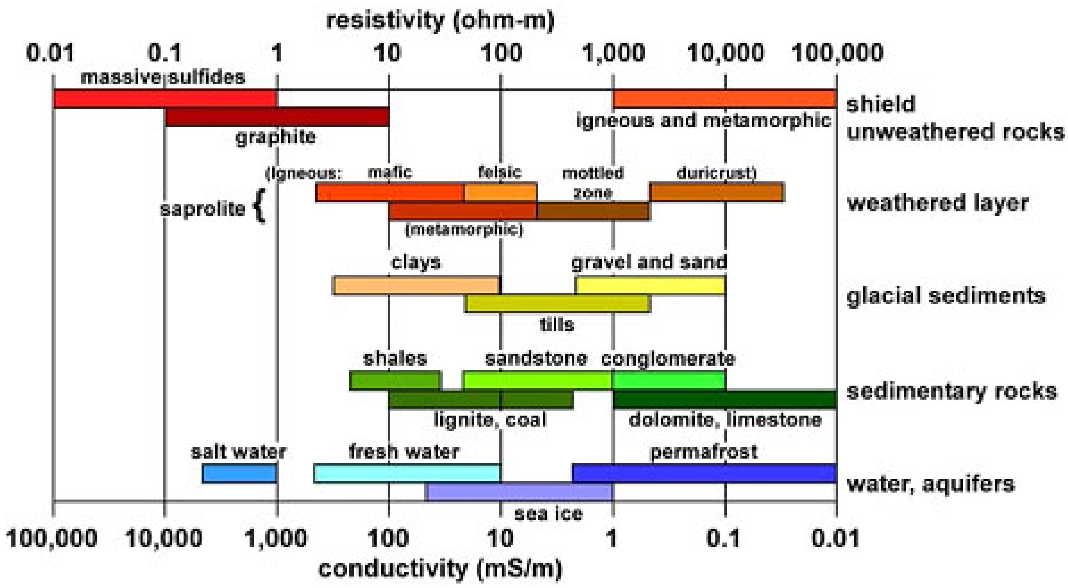

Figure 3 Typical ranges of electrical resistivity (ohm-m) or conductivity (mS/m) for selected Earth materials (based on Palacky 1988)

2.3 AEM datasets for the northern Eyre Peninsula

As part of G-FLOWS Stage-2, we have negotiated access to, and reviewed many of the available AEM datasets for the northern Eyre Peninsula. Different systems used for data acquisition are grouped by colours (see Figure 1), which indicate AEM data distribution over mapped regolith materials including potential aquifers. Without geophysics, the vertical and horizontal extents of aquifers cannot always be easily predicted from surface geomorphology or terrain analyses.

2.4 The importance of proper modelling

Forward modelling refers to the process of calculating a response given a physical property model. Inverse modelling or inversion is the reverse operation to forward modelling, and attempts to derive a physical property model given a set of observations (discussed in section 3.1 and 3.3). Examples in the literature (Christiansen *et al.* 2011, Ley-Cooper and Munday 2013) have shown some of the consequences of inaccurate description of AEM systems and how those inaccuracies influence forward modelling. Some of the most crucial parameters that are fed into the modelling are the system's geometry, the altitude of both transmitter-receiver (Tx-Rx), the shape of transmitted EM pulse (waveform), and the integration of the signal over the width of the receiver time gates (in the case of time-domain systems).

All systems have intrinsic peculiarities which need to be identified and defined to allow consistent results from the modelling. The project has inverted 17 different legacy datasets which have been acquired over different periods of time. A graphical representation of the AEM systems modelled in this work is shown in Table 1. The table presents a condensed way of visualising the different Tx-Rx system geometries and enables comparison of the main differences between the systems.

Table 1 - Specifications of AEM systems used to acquire data over the northern Eyre Peninsula (SA).

	TEMPEST	VTEM	VTEM MAX	HOISTEM	REPTEM
	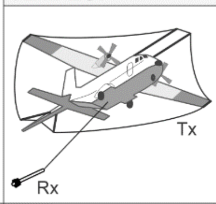	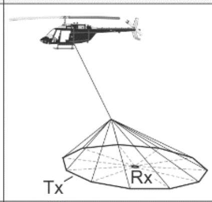	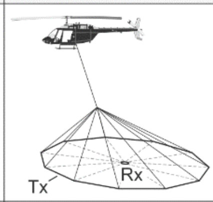		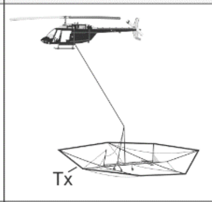
Survey Year flown	2006, 2007, 2008	2011	2014	2006	2010
Platform	Fixed wing	Helicopter	Helicopter	Helicopter	Helicopter
System geometrical configuration	Transmitter (Tx): Loop on aircraft	Concentric loop Tx/Rx	Concentric	Concentric	Concentric
	Receiver (Rx): Towed bird	Suspended weight	Suspended weight	Suspended weight	Suspended weight
Nominal heights Tx	Tx: 120 (m)	Tx: 49 (m)	Tx: 54 (m)	Tx: 30 (m)	Tx: 30 (m)
Rx	Rx: 65 (m)	Rx: 49 (m)	Rx: 54 (m)	Rx: 30 (m)	Rx: 30 (m)
Transmitter coil axis	Vertical	Vertical	Vertical	Vertical	Vertical
Tx loop area	186 (m^2)	531 (m^2)	962 (m^2)	300 (m^2)	375 (m^2)
Tx base frequency	25 (Hz)	25 (Hz)	25 (Hz)	25 (Hz)	25 (Hz)
Tx number of loop turns	1	4	4	1	1
Peak current	300 (A)	200 (A)	243 (A)	320 (A)	340 (A)
Peak moment	55,800 (Am^2)	424,740 (Am^2)	861,952 (Am^2)	180,800 (Am^2)	127,000 (Am^2)
Nominal waveform shape	Quasi-Square	Half Sine-Trapezoid	Half Sine-Trapezoid	Half Sine-Trapezoid	Half Sine-Trapezoid
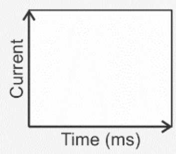	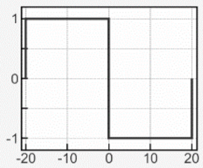	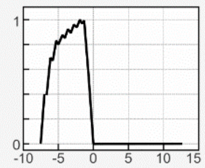	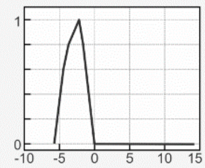	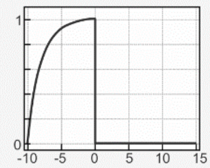	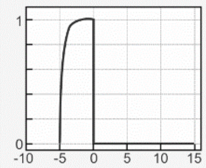
Duty cycle	50%	37%	37%	25%	25%
Tx height measured	Measured	Not measured (derived from helicopter)	Derived from helicopter	Measured	Measured
Tx orientation	Measured (from aircraft)	Measured Indirectly (GPS)	GPS	Not measured	Not measured
Tx-Rx separations	Not measured Nominal horizontal 100 vertical 53 (m)	Not measured (flexible frame)	Not measured (flexible frame)	Not measured	Not measured
Receiver orientation	Not measured	Not measured	Not measured	Not measured	Not measured
Receiver coils	X, Z & (Y not delivered)	X & Z	X & Z	Z	Z
EM Sensor	dB/dt	dB/dt	dB/dt	dB/dt	dB/dt
# of receiver windows	15	35	45	21	22
EM channels start times (ms)	0.007 to 12.4 (ms)	0.078 to 8.6 (ms)	0.018 to 9.9 (ms)	0.066 to 10.7 (ms)	0.065 to 12.9 (ms) YLf001-14

2.5 System differences, variations and their implications

Modelling coincident loop VTEM systems used over some extensions of the total survey area has provided an example to demonstrate some of the implications of improper parameter consideration when modelling.

In order to model a relatively newer $VTEM_{max}$ system, which we had not used before, the considerable differences to its contemporary $VTEM_{508}$, system needed to be considered. The newer $VTEM_{max}$ system samples the decay over more receiver gates, has a higher peak-moment and its waveform has a different shape. The particular differences between these systems can be identified in Table 1.

Using the systems' specifications provided by the contractor (Table 1), we modelled two generations of the same AEM system (Figure 4). This figure shows the response from both a resistive (EC of 0.001 S/m) and a conductive (EC of 1 S/m) synthetic homogenous half-space. The geometry of the input or transmitted waveforms (left panels of Figure 4) is clearly different. This difference, despite the fact that current has been normalised, makes both curves appear as if they were of similar amplitudes. The newer system (in grey circles) samples the decay over more windows and earlier in time, implying it might be better for resolving structures in the near surface.

The response of the higher powered $VTEM_{max}$ system over the resistive half-space presents an unusually non-monotonic decay pattern in its early times. This could be the result of improper system description, or alternatively it may be that further sampling and post-processing artefacts like digital filters need to be reported in order to appropriately model the new early times. Further work is needed to resolve the reason for this decay pattern.

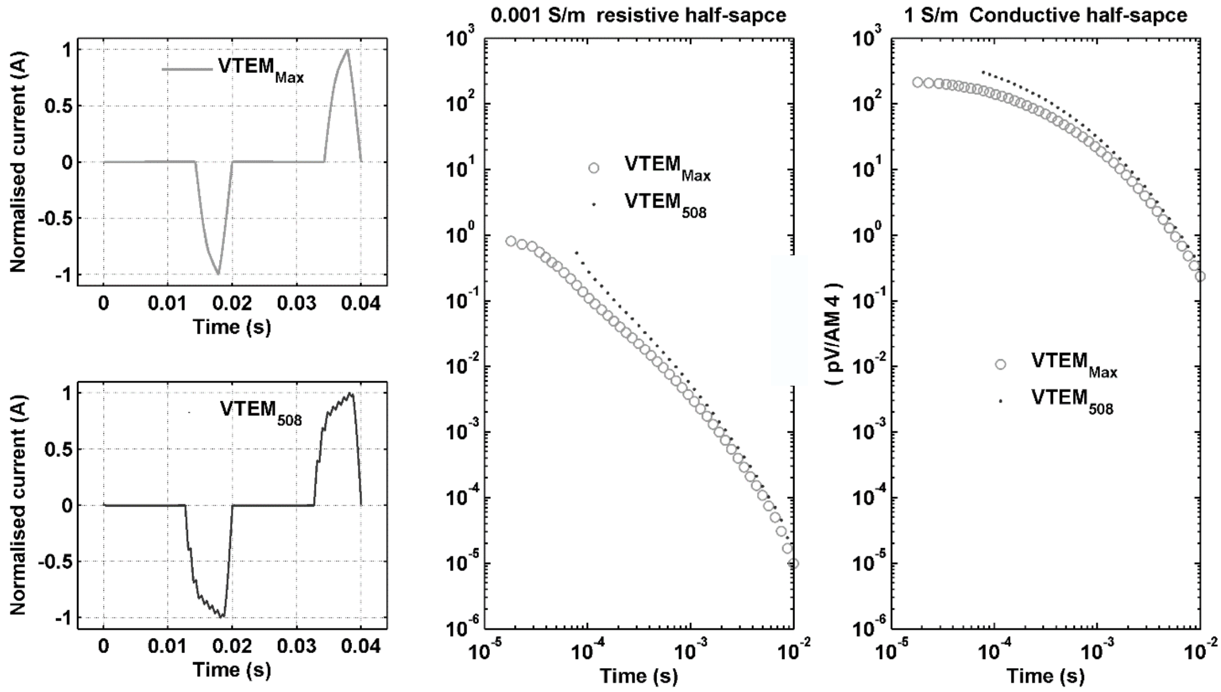

Figure 4 - Waveforms from two generations of a VTEM system on the left panels. The response (dB/dt amplitude) of these two systems over a resistive and a conductive half-space is shown in the right panels.

What has not been included in the two right-hand response plots is a noise model, which is known to vary at every location due to changes in both geology and survey conditions. Without a noise-model correction measurement we cannot make an objective assessment on the systems depth of investigation capabilities, despite intuitively assuming the higher powered system would penetrate deeper.

For these two particular systems the transmitter (Tx) and receiver (Rx) heights are not measured directly, but have been derived through trigonometry using the reported measurements from the helicopter. In some cases, particularly when dealing with older data, the cable length used to carry the transmitter (Tx) loop as a sling load beneath the helicopter is not provided, which also increases the uncertainty of the modelling.

3 Inversion of raw data

In order to investigate the available raw AEM datasets, geophysical inversion has been used as the approach to review the data and propose models of conductivity and depth.

Extracting conductivity and depth models from the measured AEM data is a procedure that is done by either approximate conductivity-depth-transforms (CDT) or by inversion. Practical electrical conductivity transformations are restricted to those employing a 1D approximation for each recorded location. Measurements taken at each location are treated in isolation from those obtained at other locations. The ground is assumed to show electrical conductivity variations in only one direction (i.e. along a vertical axis), and hence all conductivity layers are infinite in horizontal extent. Inversions provide an EM model response that corresponds to the proposed final conductivity-depth model. Goodness-of-fit metrics enable a quantitative appraisal on the level of agreement between the proposed model and the measured data. Both standard deterministic inversion (section 3.1) and stochastic inversion using MCMC analyses (section 3.3) have been applied to all five AEM data sets listed in Table 1.

By stitching the inverted 1D samples together we build a conceptual 3D conductivity structure, which we slice and present as maps and sections for interpretation. A work flow illustrating how this is done is represented in Figure 5.

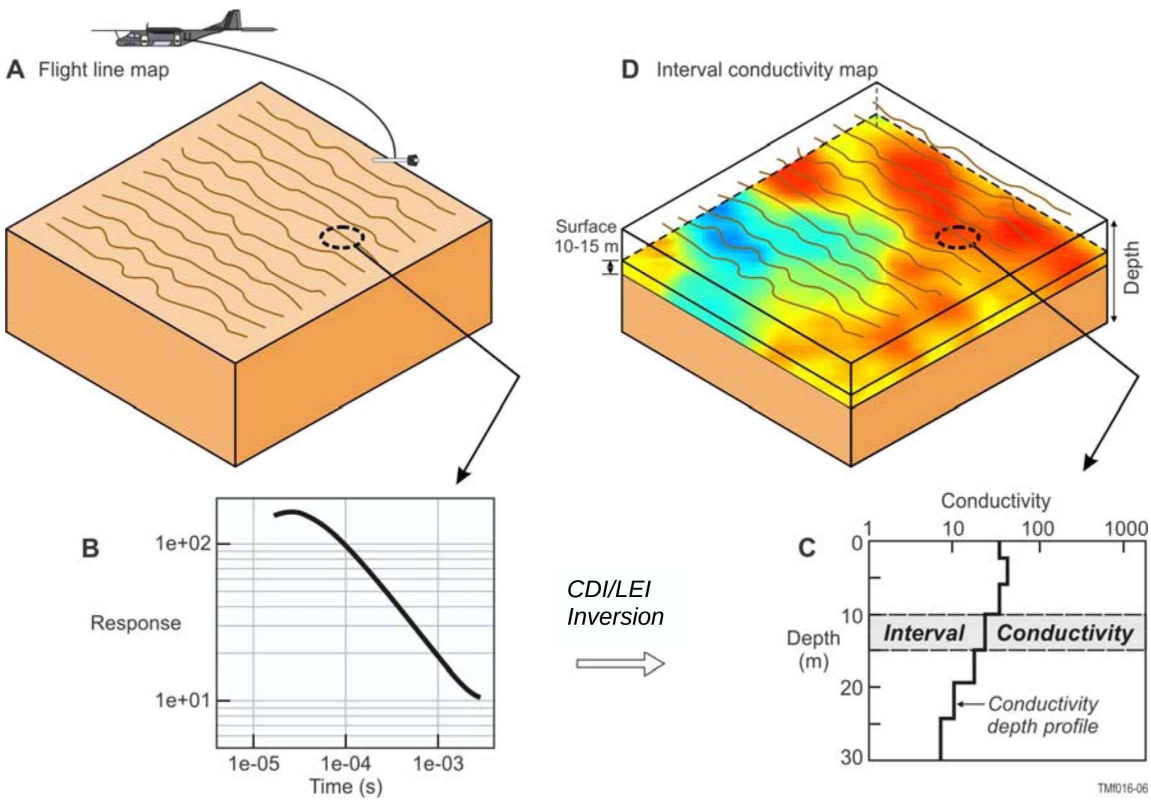

Figure 5 - AEM workflow from acquisition to interpretation (CDI) of derived products (adapted from Fitterman and Deszcz-Pan 2001). CDI = Conductivity Depth Inversion; LEI = Layered Earth Inversion.

3.1 Standard deterministic inversion: principles and application

The 17 available AEM datasets in the northern Eyre Peninsula were processed, inverted and analysed by applying a common algorithm which transforms raw AEM data into layer models of conductivity and depth. Geoscience Australia's 1D layered-earth sample-by-sample (SBS) inversion (GA-LEI) method developed by Brodie et al. (2004) was used. Deterministic inversion methods output a single optimum solution, and this one has an inbuilt iterative optimisation function. The SBS inversion is also called a smooth layer inversion, where the thickness of each layer is fixed and the values of conductivity are allowed to vary and be resolved by the inversion scheme.

Sample lines of data were inverted by changing the parameterisation and using different starting models, which involves estimating the depth of regolith layers and their estimated conductivity. After various trials the better fitting models were selected. Because of the lack of noise measurements, noise estimate levels from previous surveys have been used. Despite the overall satisfactory fit for most of the data, in some surveys particularly the late time channels are poorly fitted. Some of the poor fits are artefacts of an inversion that is trying to fit negative data, which is unusual (although possible over very resistive terrains or in areas with potentially big induced polarisation (IP) effects). In this particular case, it is believed to be attributable to data noise.

For illustration purposes, a flight line from each system flown is shown in the following sections and the inverted data as a profile section of conductivity and depth is displayed. In order to extract meaningful hydrological information from these 2D profiles, they need to be looked at in a geographic context. Location in the landscape and the associated mapped surface material can allow inferences to be made – for example, the lines flown close to the coast line (such as the right side of Figure 9), the identification of salt water intrusions becomes quite obvious. Over locations where boreholes were available, we have projected the drill logs on the AEM profiles in order to try and determine whether there were possible conductivity-lithology correlations.

3.1.1 HOISTEM

One survey using the Hoistem system (Boyd 2004) was available in the NW of the study area (see Figure 1). The survey was flown on the north western part of the Eyre Peninsula. These data were acquired in the exploration of palaeovalley uranium. The derived section shown in Figure 6 identifies two main disconnected flat-lying bodies: one between 4000 - 6000 m from the start of the line in the east, and a second much larger body from around 7000 - 15 000 m from the start of the line. These bodies are composed of conductive material (~1000 mS/m) at around 150 m depth. The distribution and shape of these bodies suggest this conductive response is from a combination of conductive sediments and more saline ground water, although knowledge of the exact material will require underpinning ground-truthing.

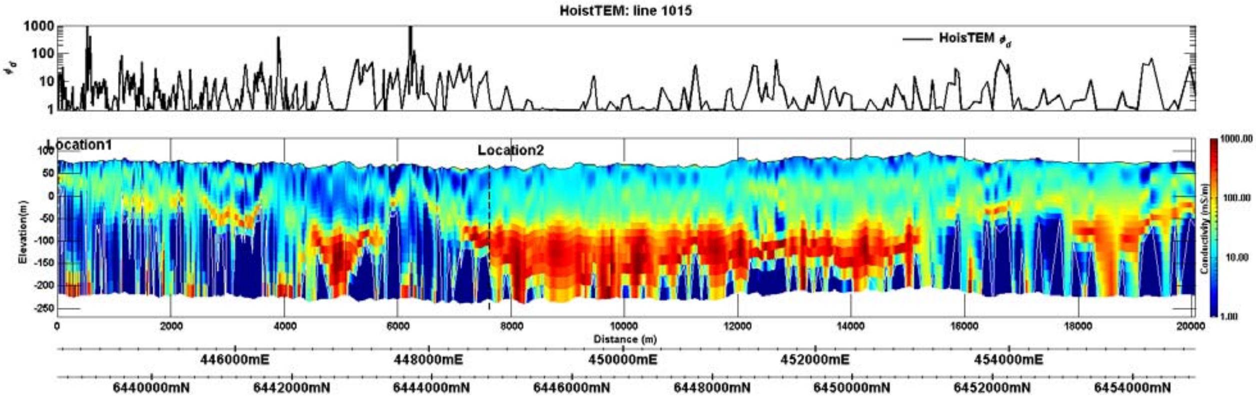

Figure 6 - Line of inverted Hoistem data. The top Panel shows misfit parameter φ_d, which is as an indicator of how well the proposed layered earth models are representing the acquired data at each sounding point. When numbers are closer to 1 there is better correspondence. The bottom panel shows a 30-layer conductivity section determined from a sample by sample (SBS) inversion.

Detail of two decays and their respective conductivity depth models at two locations reveals issues with the measured data at late times. This can be seen in detail in the bottom panels, where the two modelled decays (in magenta) are trying to fit spurious data (black) at later times. As a consequence the inversion places a very conductive body at depth. The Hoistem is a low-powered system hence there is limited expectation of it resolving structures at great depths, and it is particularly noisy over resistive ground. The precise depth that this method is useful depends on the conductivity of the ground, but is less than other more powerful systems.

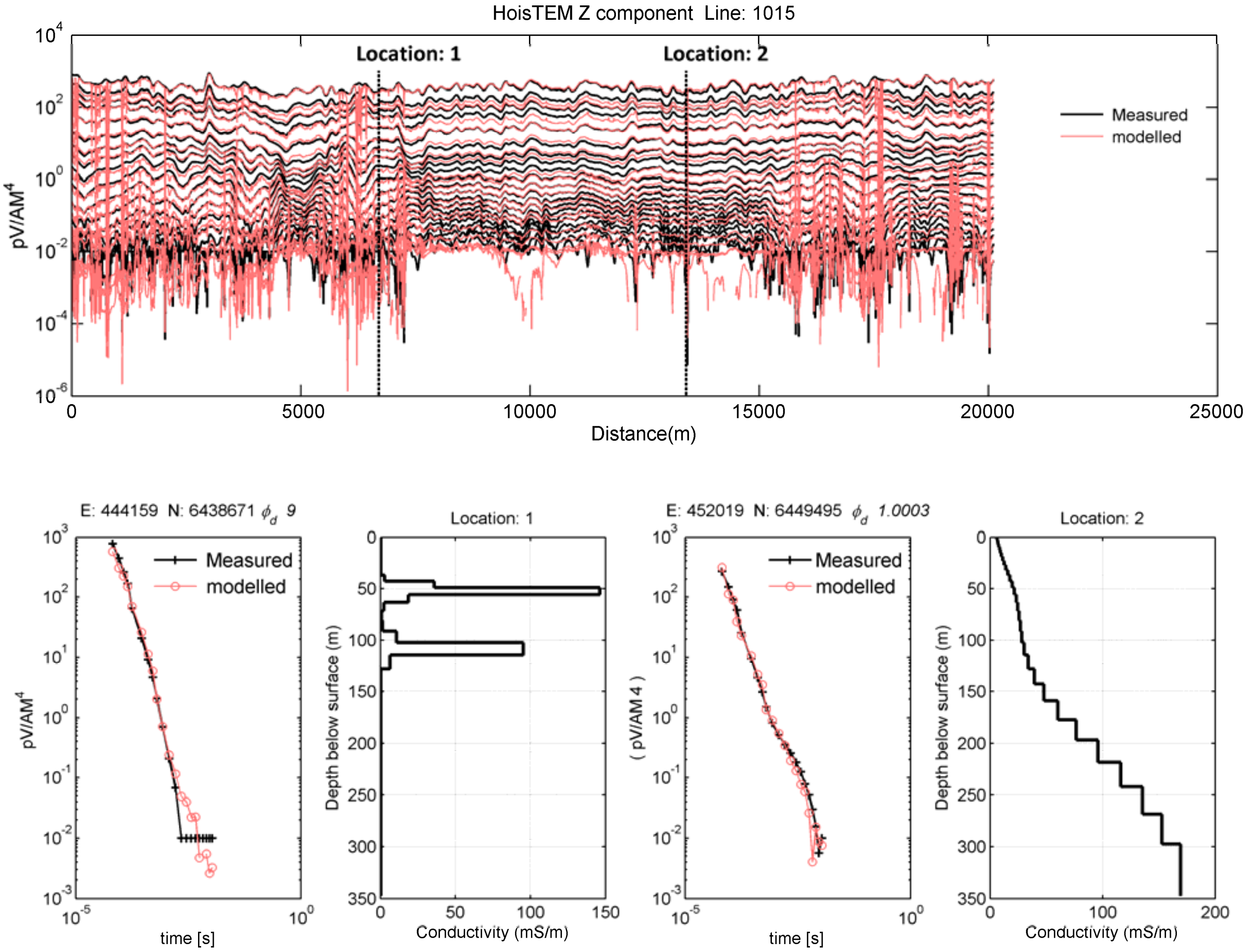

Figure 7 - Top panel shows the measured (black) and modelled data (red). Bottom panels show measured and modelled decays (TEM response) at two locations and their associated conductivity-depth model.

3.1.2 TEMPEST

TEMPEST data was also collated by the project team, and despite spanning over a range of years, the data is very consistent in terms of its delivered method and quality. The top panel in Figure 8 is an indicator of the level of agreement between the measured and modelled (GA-LEI 30) data. High values of ϕ_d, are usually indicators of locations with spurious data, or steeply dipping boundaries with strong 2D and 3D effects on the data which cannot be appropriately resolved with the 1D algorithm that has been employed. The bottom panel shows a fast transform (Conductivity Depth Inversion - CDI) section generated provided by the contractor using EMFlow (Macnae *et al.* 1998). Above it is the GA-LEI 30 smooth layer inversion which has a finer vertical resolution and is able to resolve finer details in the regolith.

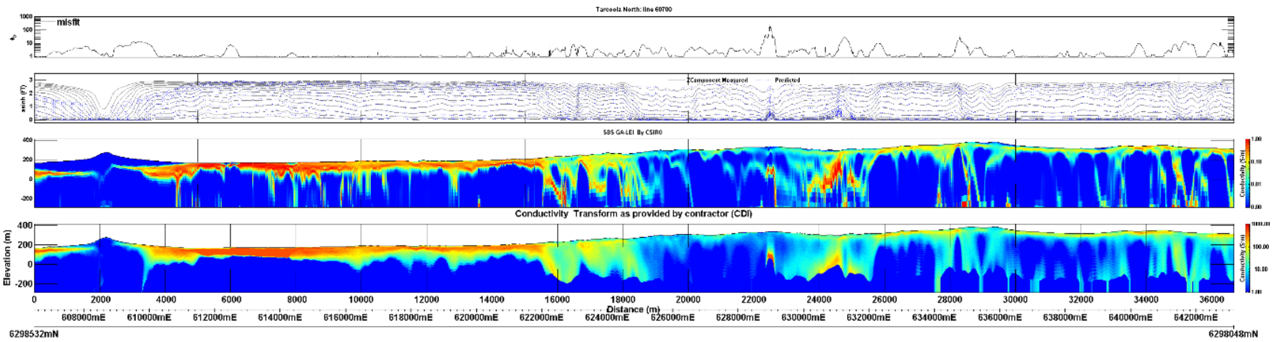

Figure 8 - TEMPEST line showing a comparison between the conductivity models provided by the contractor and inverted data. The top panel shows the level of fit at each location as a profile. The second panel show the raw Z component channels of EM data displayed as a continuous streamed profile in grey and the modelled channels in blue. The third panel shows the GA-LEI inversion transect. The fourth panel shows the original conductivity transform provided by the contractor.

The 2D conductivity profiles shown in Figure 8 highlight some important differences that should be noted between the CDI fast transform (top 2D profile) and the inverted model (bottom 2D profile):

- Around 2500 m from the start of the flight line on the left, there is a flat-lying intrusive conductor (pale yellow/green band which stands out from the blue). The inversion resolves it under the hill whilst the transform places it at the surface.
- At ~22 000 m from the start of the line there is a confined conductive body which is resolved both in the transforms and the inversion, which would be worth following up with ground-truthing in future work.
- At ~24 000 m from the start of line there is a conductive body. It is unclear what this is, although it could possibly be associated with structural movement (a fault?). Its dimensions and geometry appear to be better resolved in the inverted data. These types of hidden structures are of interest from a hydrological perspective since they can influence groundwater flow, and would benefit from future ground investigation to determine their cause.

In some locations, profiles have been constructed by slicing conductivity–depth models to intersect places with logged borehole lithology (Figure 9). A direct correlation between the conductivity layers and lithological units should not necessarily be expected for several reasons:

1) The resolution of a fixed wing AEM system like TEMPEST, at surface is an annulus with a diameter over a 100 m at surface (Ley-Cooper *et al.* 2010). It samples several thousand square metres at increasing depths. In contrast the recovered core from a borehole has a diameter of tens of centimetres at the most. Differences between the scales are expected, and determining the scale of differences forms part of the uncertainty of the predictions.

2) Conductivity models derived from airborne EM data are always approximations of the true conductivity-depth distribution. The number of layers used to construct these models generally is lower than the number of existing lithological units. Therefore an AEM model-layer often represents several lithological layers. Particularly where several small layers are interbedded, AEM would provide an average of this small-scale variation.
3) Direct stratigraphic interpretation of conductivity is only possible when there is a sufficient lithological variation that can be correlated with a strong change in conductivity. If bores are present, it would be possible to provide aspects of this information with borehole geophysics to determine EC.

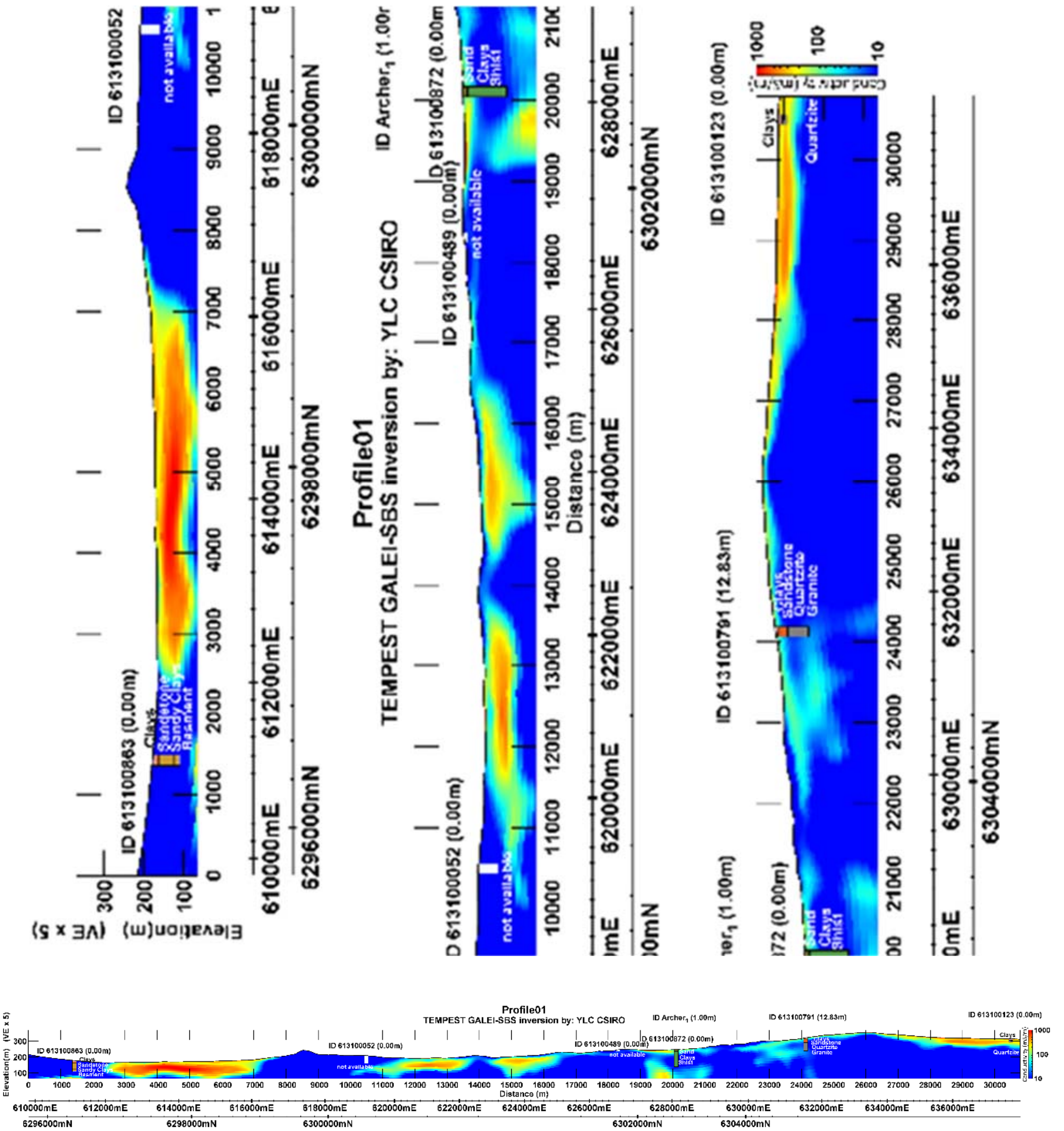

Figure 9 - Profile generated by slicing the constructed 3D conductivity-model, to intersect shallow boreholes with logged lithologies. (from left to right: Profile has been separated into 3 sections (lleft, central, and right parts of the same profile). Full profile is shown across the bottom panel.

3.1.3 REPTEM

The Reptem system is in essence a second generation higher powered Hoistem system. For the modelling of this work, additional data was available in the form of flight lines acquired over the ocean. For these lines the ocean's conductivity was measured from a helicopter-dipping a conductivity probe (Vrbancich 2011). This provides a verified point of calibration for the AEM data.

No estimation on the sensitivity of the instrument was available from data collected on the original surveys, hence no real noise-model could be developed which is a critical requirement for modelling. Vrbancich (personal communication) performed a series of test on the system around the same time of acquisition of some of the surveys and provided us with estimations of the noise-levels for each channel.

The results are shown in Figure 10. The top panel has again a profile of parameter ϕ_d, which is calculated and use as an indicator for assessing the level of fit between measured data and the models derived from inversion. The lower values of ϕ_d, reflect a better agreement between models and measurements. For this line two distinct domains can be drawn. The right part from the section (coastal plain) shows a good correlation over the areas where the system has measured a response with higher signal. The left side from the section (resistive rocks) has a very low signal and hence the derived conductivity models tend to be poor. There is a suggestion of some near surface conductors - maybe regolith related, although the deep conductors are noise and not signal. With a model misfit of >>1 in this area, this suggests that modelling the data across a range of conductivity structures can be challenging, and may be problematic, particularly where basement is present at the surface.

The middle panel shows all measured channels of the Z vertical component as a continuous streamed profile in grey. The equivalent modelled channels are overlaid and plotted in blue. This middle panel reveals several dropouts along the line, particularly over mid part of the section from ~4000 - 9000 m from the start of the line on the left. In these areas the conductivity section shows some evidence of a poorly defined mild conductor at surface which can also be seen on the bottom panel.

On the right of the profile from 10 km onwards a saline plume is nicely mapped and modelled with high fidelity. Its extent and morphology can be easily determined by the contrast in conductivities. The coastline is the right edge of the profile (distance ~16 400 m), and the plume (red) extends away from the coast getting gradually deeper over several kilometres under the coastal plain.

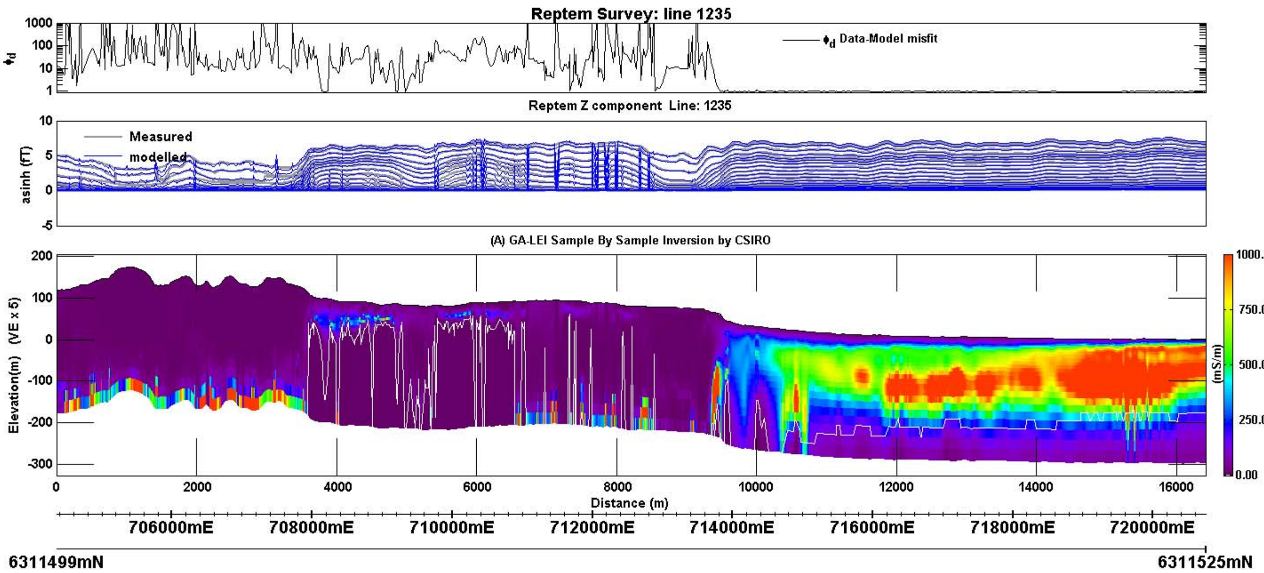

Figure 10 – Reptem results. Top panel shows parameter ϕ_d, an indicator of the level of agreement between models and measurements. Middle panel shows all measured channels of the Z vertical component (grey) and the equivalent modelled channels (blue). A conductivity depth profile is displayed in the bottom panel.

3.2 Standard deterministic inversion: effect of inversion model

3.2.1 VTEM

In the west coast of the northern Eyre Peninsula, between Elliston and Venus Bay (see Figure 1), a VTEM system was flown in 2006. In the area there are independent water supply schemes, which are tapping sources of local isolated freshwater lenses located in the Quaternary aquifers (Risby and Harrington 2014).

The flight-line distribution and a derived map of the inverted conductivities at a depth of 20 m below the surface have been draped on a derived surface topography layer (MrVBF: Gallant and Dowling 2003). In Figure 11 the paler grey colours are indicative of low flat areas in the landscape. Darker grey areas are steeper and higher parts of the landscape. MrVBF provides insights into consistently low and flat parts of the landscape, which can be associated with filled valleys and old drainage lines.

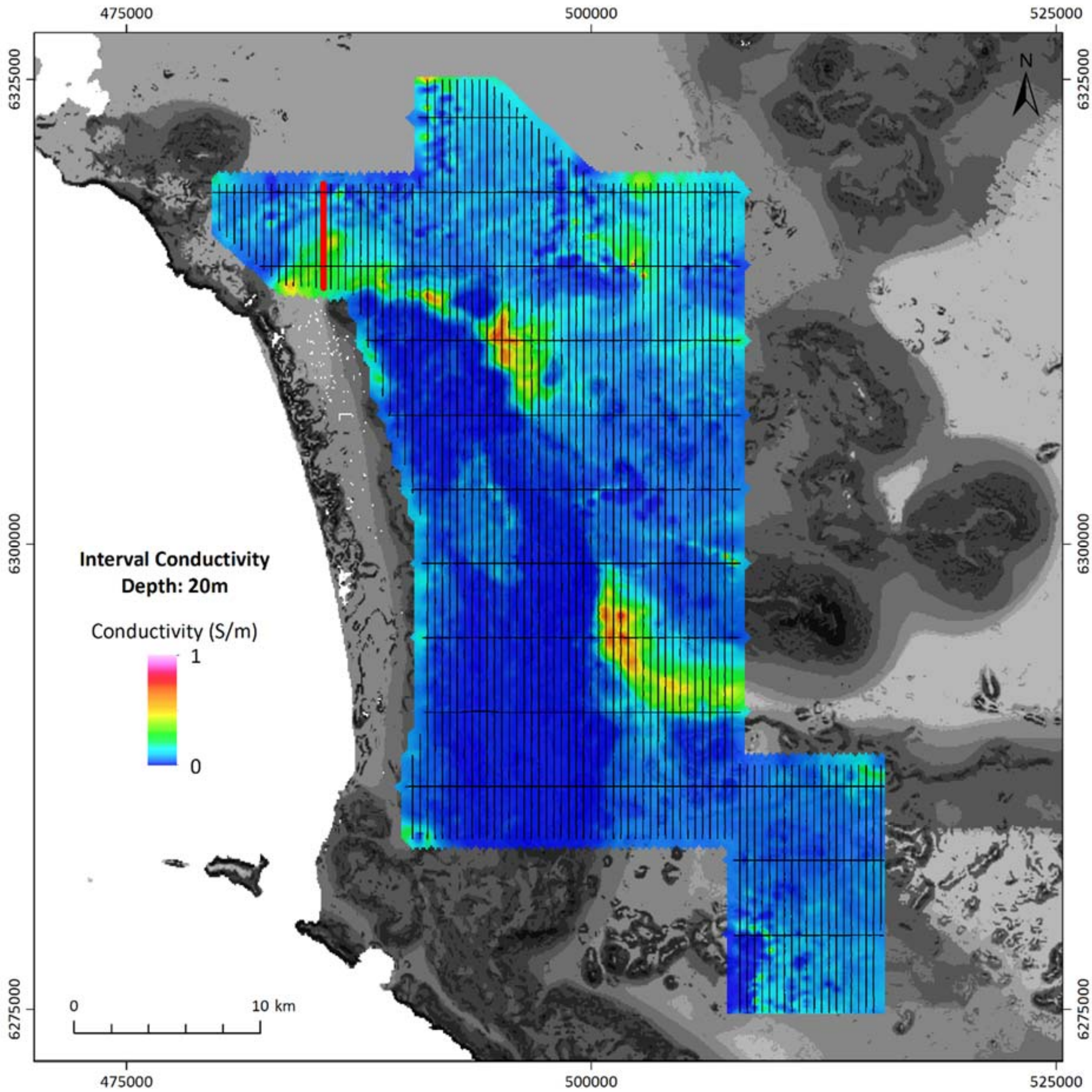

Figure 11 - A map of conductvities at a depth of 20 m below surface which has been derived from inversion. VTEM Flight paths are overlaid as thin black lines. As a back drop in grey-scale, is a terrain analysis map derived from surface topography (pale grey = low and flat, dark grey = high and steep).

Information about the altitude of the transmitter and the instrument's noise levels was not available for this dataset. Therefore, we applied a series of assumptions and trials to derive what appear to be adequate and credible parameters. The assumptions included – nominal flying height of the system above the ground (system geometry) and noise levels of the system flown. Indicative estimates of noise were derived from previous surveys flown with the VTEM system, although it is recognised that this can be system specific.. As a trial exercise, we have recovered a series of inversion models on one same line of data. A flight line of data was scrutinised from the north western part of this survey, which is highlighted in red in Figure 11. The line was selected as an example, since it identifies what could be potential small fresh water lenses, like the ones currently sourced in the area as local water supplies (Risby & Harrington, 2014), and includes what we speculate is the front of a salt water intrusion.

3.2.2 MULTIPLE OPTIONS

The GA_LEI inversion method uses what is known as gradient-based optimisation technique; this is a local optimisation method. It minimises an objective function comprised of data misfit and model regularisation. The inversion looks for a single 'best' model through an iterative processes, using an optimisation function that fits the data within established noise levels. A limitation of this approach are that if your guessed conceptual model of a geological structure and a related conductivity is extremely poor, this can force the gradient- based method to give you an equally weak model of the conductivity structure. This disadvantage of the gradient-descent algorithm is that it will can get trapped in a local minimum if the starting model is too far from the globally optimal solution (Figure 12), so care must be taken when selecting starting points for the optimisation. Other approaches such as stochastic ones have the flexibility to explore model space more effectively, and can use information from drill hole conductivity logs, or ground EM data to better constrain the model, but at the price of a large computational overhead.

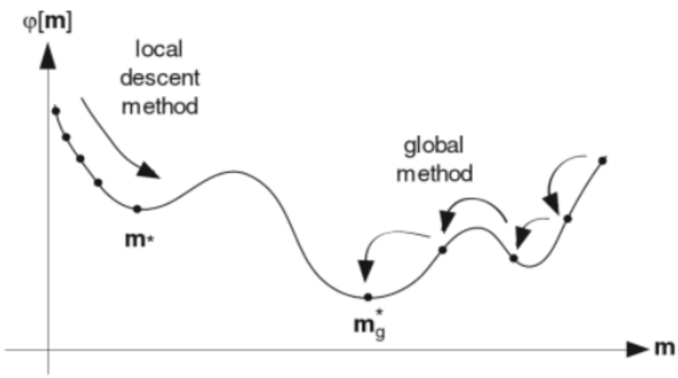

Figure 12 Local optimisation methods such as the gradient-based approach only find a local minimum m* of the objective function. Global methods such as MCMC can jump out of local minima and find the global minimum m_g*. (Source: Everett 2013)

Changing constraints

One option is to change the "smoothness constraints" in the inversion, a parameter that imposes the level of vertical variation or transition between overlying layers. This "smoothness" is implemented through a dimensionless number; high smoothness numbers mean that the change is slow between layers, and the lower the number, the more quickly conductivity is allowed between modelled layers.

The interpretation process is limited to establishing the electrical conductivity of the layers. The term smooth model is owed to the fact that resistivities change very gradually from one layer to the next. One of the primary advantages of smooth inversion is that it is often possible to identify complex geological structures such as inclined layer boundaries, which are hard to detect when using fewer layer models. The disadvantages of smooth inversion are that in some contexts layer boundaries are diffuse and that the depth of investigation is unknown. The

The same line of data was inverted multiple times, using a 30-layer model, each with different smoothness. The results are then compared as stack in Figure 13. The recovered sections show clear distinct vertical variations. The most striking contrast is between the joltier less-smooth bottom section and the very smooth slowly varying section on the top panel.

One of the common features for all three sections is in the conductive wedge on the right-hand side of the section (thin red area under the "Location 4" label in Figure 13). The red line appears to be mapping the saltwater intrusion front in the southernmost part of the profile (see southern end of red transect line shown in Figure 11). The differences between the sections are many but a noticeable one is between 3000 - 3500 m from the start of the line on the left. At this location the presence of a less conductive feature (possibly a fresh water lens) seems to be mapped on both the middle and bottom sections (shown as a blue section in the 3000-3500 m part of the profile) but is absent on the top section (which shows all green) that had smoother constraints imposed.

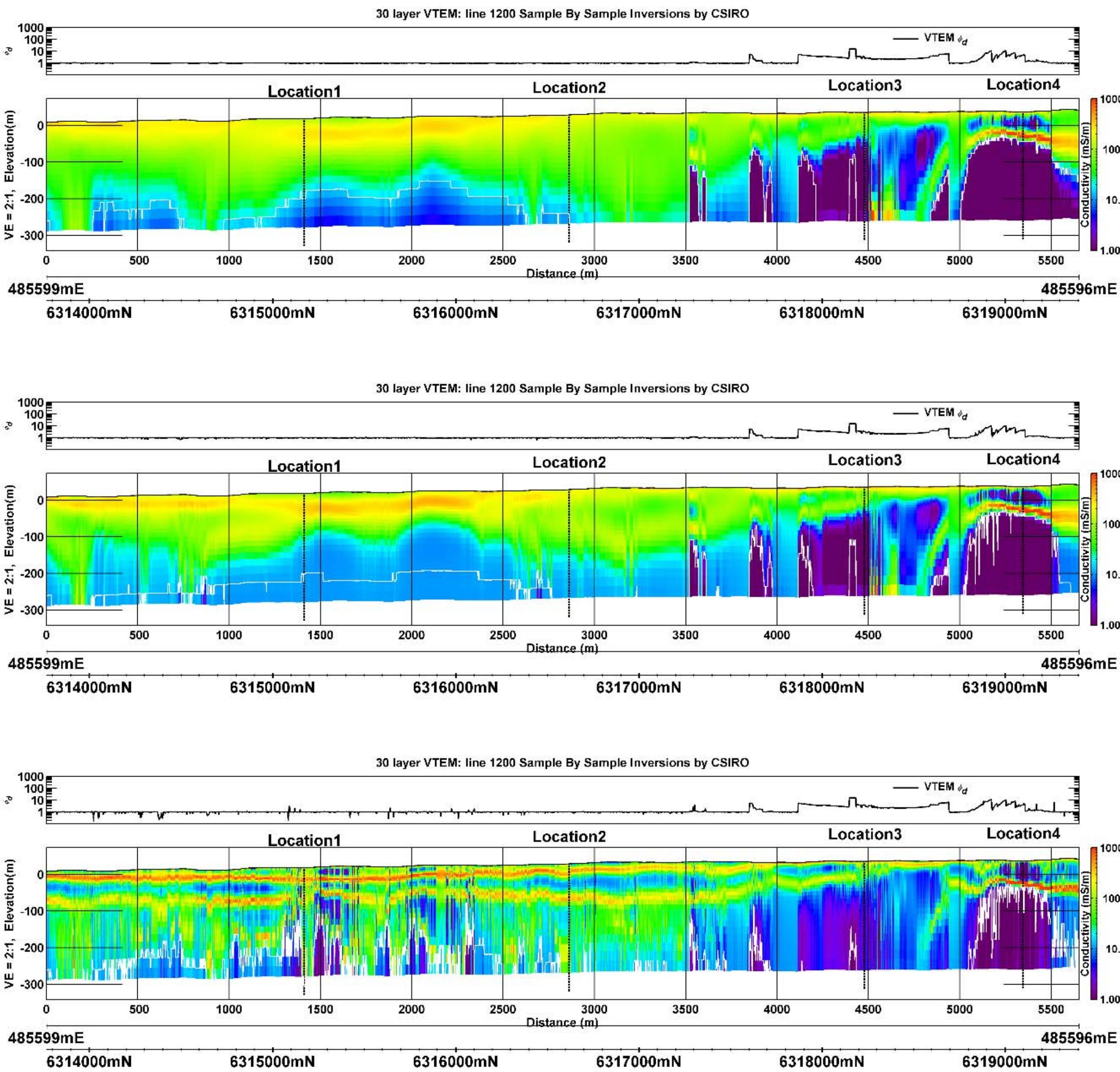

Figure 13 - Sections with different vertical conductivity smoothing. Top panel has the highest smoothness, the middle panel has a medium smoothness, while the bottom panel has a low smoothness. The faint white line at the bottom of each section is an estimated depth of investigation calculated at each location.

A way of further inspecting the modelled results for these inversions is to compare the measured and modelled results in areas where there are major differences. In the smooth section (Figure 14) and jolty section (Figure 15) we have selected the same four locations along the line to assess, their decay-curve responses and models, in an individual manner. Note that both proposed models have a similar level of fit, which suggests that the inversion has identified two sections that are equally able to represent the response observed in the measured data. From this analysis alone, there seems to be no real elements that favours one inversion over the other. Clearly, the inverse problem is highly underdetermined and results in many non-unique solutions. This calls again for the need to incorporate independent field observations to better constrain the inversion process.

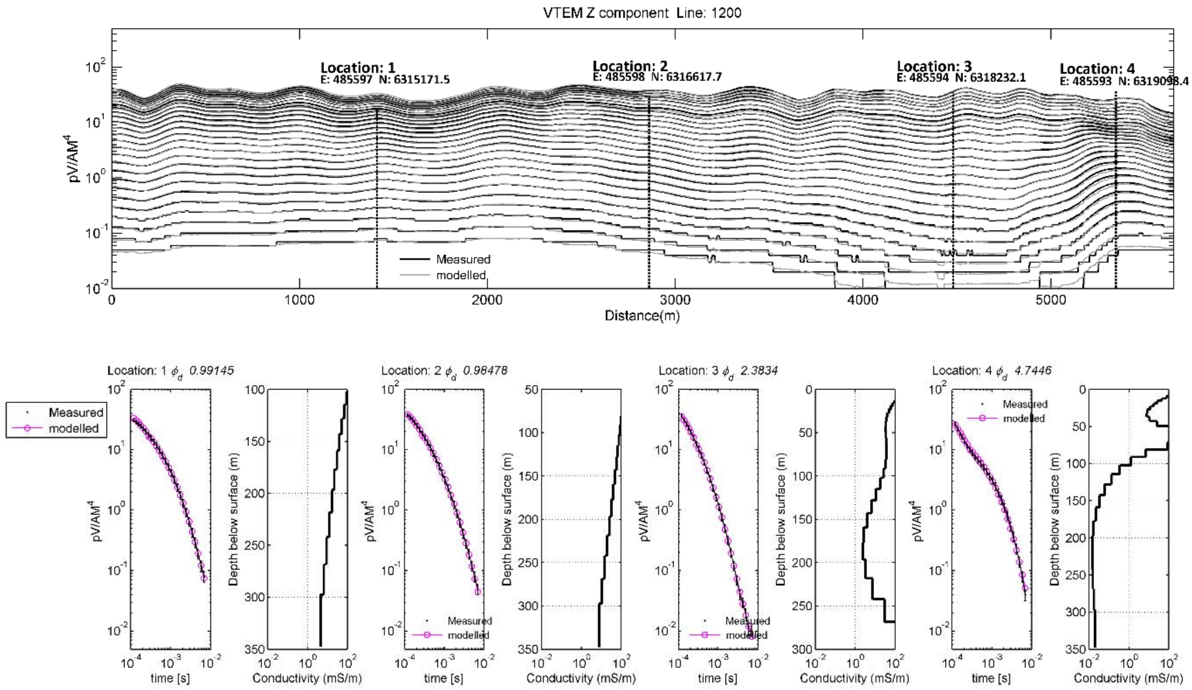

Figure 14 - Vertical smoothing 1 000 000 (= fine layering). Top panel streamed channel of measured and model data for the whole line. Bottom panels 4 individual measured and model decay-curves at different locations, and their associated derived conductivity-depth model.

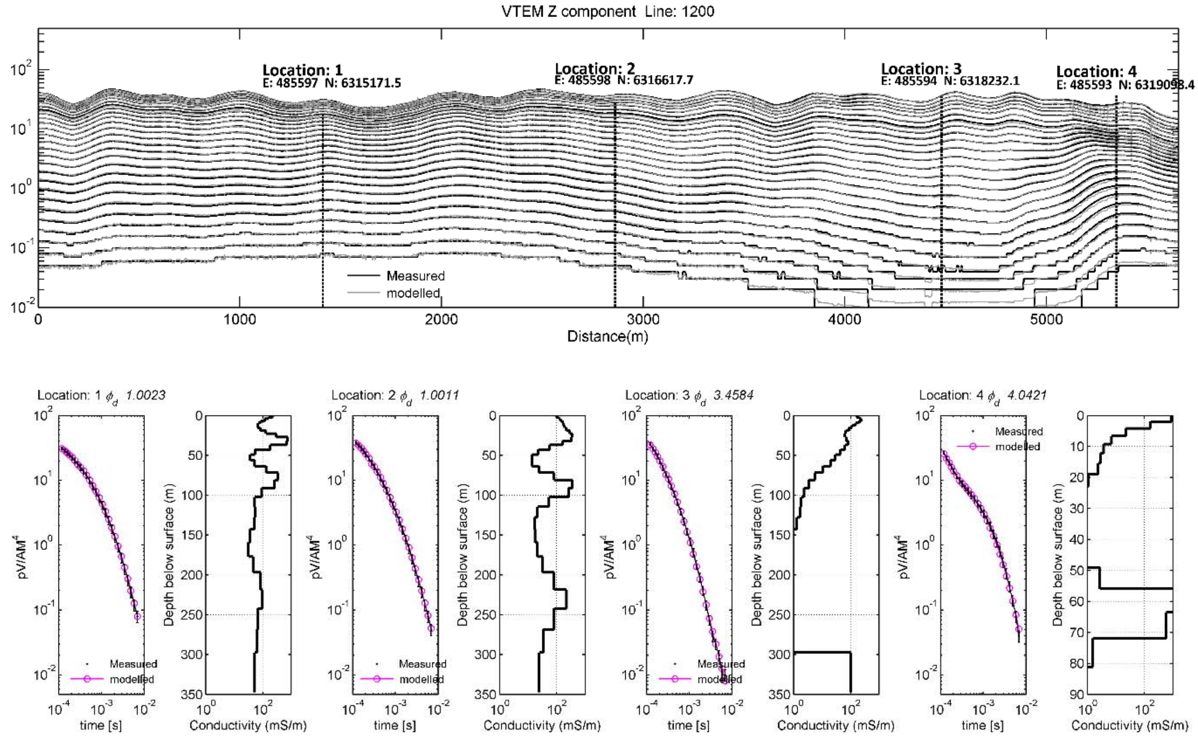

Figure 15 - Vertical smoothing of 100 (= coarse layering). Top panel streamed channel of measured and model data for the whole line. Bottom panels 4 individual measured and model decay-curves at different locations, and their associated derived conductivity-depth model.

Solving for depth

The inversion results presented so far in this report have been resolved using a 30 layer sample-by-sample (SBS) inversion, also referred to as smooth layer inversion. The thickness of each layer is fixed and the values of conductivity are allowed to vary and are resolved by the inversion.

The option of solving for both layer-thickness and conductivity poses a higher degree of conflict between choosing a representative model. Figure 16 and Figure 17 show results for the same VTEM line, but solving for a 12 layer and a 5 layer model, respectively. As in the previous example with the smoothness variations, in this case there are also some differences between the derived models, although the overall fits for each of the models suggest they could both be equally valid. This highlights the need for AEM results to be interpreted as part of a suite of data sources, including ground-truthing using field experiments to provide more certainty on which model best reflects reality.

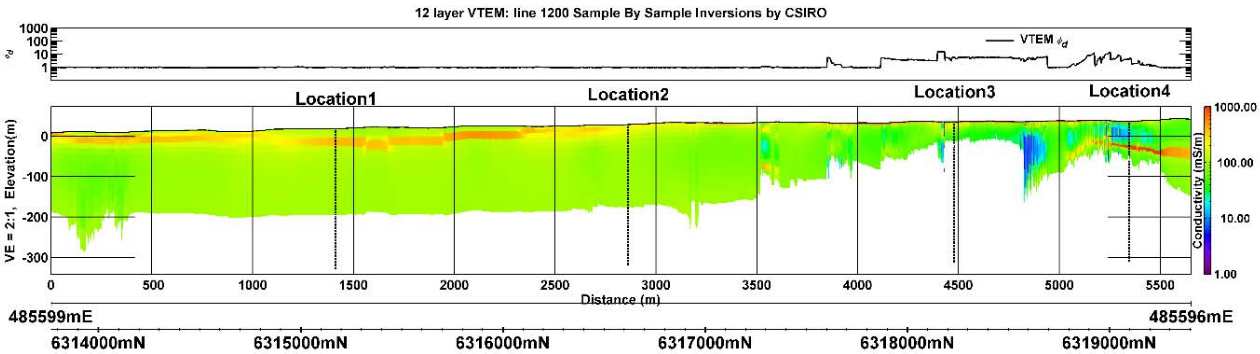

Figure 16 - Twelve layer model solving for conductivity and depth.

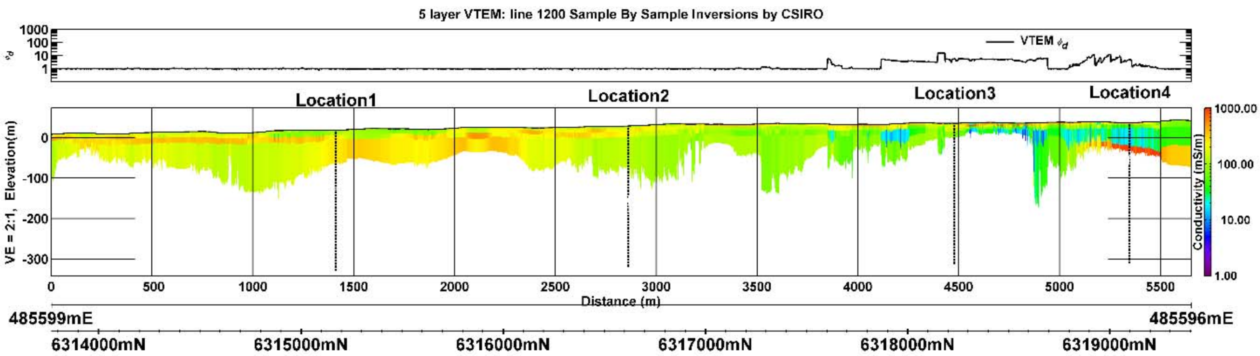

Figure 17 - Five layer model solving for conductivity and depth.

Results in Figure 18 show comparable levels of fit can be achieved by varying parameters, such as modifying the degree of vertical smoothness, layer thickness intervals, and changing the starting model for background conductivity. Varying the noise model has a greater implication which is not covered in detail here. The number of model layers and the thickness at each location are unknown, so predetermining a fixed number has imposed a bias on the level of model complexity.

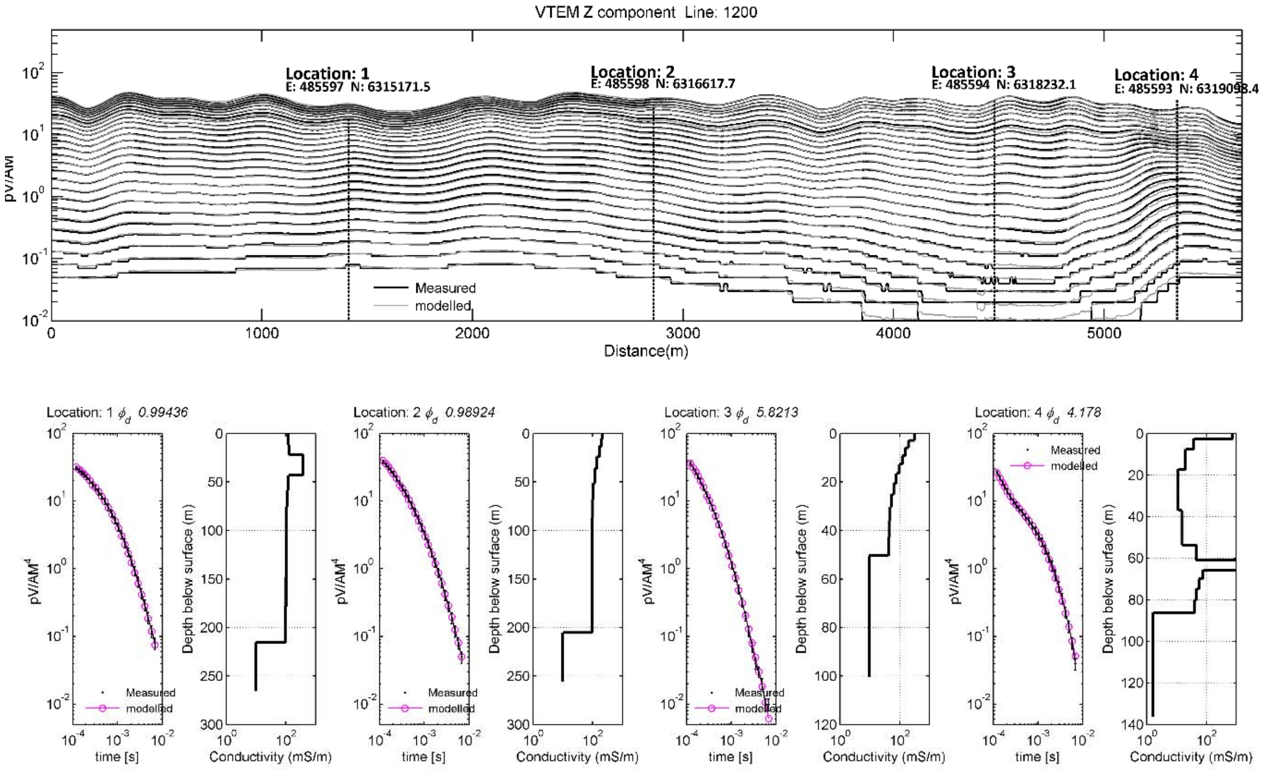

Figure 18 - Twelve layer model. Top panel streamed channel of measured and model data for the whole line. Bottom panels 4 individual measured and model decay-curves at different locations, and their associated derived conductivity-depth model.

During acquisition and under certain survey conditions, incidents like coil deformation, remanent coil response and instrumentation drift can occur. These effects that change the shape of the AEM response cannot always be accounted for. The inclusion of digital filters, the instruments' waveform and further processing of the recorded data are other considerations that can also affect the forward calculation. These are elements that could be accounted for by modelling extra parameters, with several examples found in the literature such as Schamper *et al.* (2014), Christiansen *et al.* (2011), and Davis and Macnae (2008). These unaccounted effects and undisclosed parameters all contribute to non-uniqueness of the AEM inversion problem.

Improved documentation of system characteristics for historical survey data and ensuring that these are archived with data held by the SA Geological Survey would be useful. This could include a compilation of AEM acquisition systems, their characteristics, and time frames over which those systems operated.

In terms of inversion related issues, consideration should be given to improved documentation of the consequences of varying smoothness, and the effects of other aspects of the procedures (such as filtering, optimisation approaches, noise, noise removal, etc.) to raise awareness of the effects on derived results from assumptions that are made in the processing and inversion stages.

3.3 Stochastic inversion with Markov chain Monte Carlo simulation

There are several inaccurate elements of the data acquisition and processing of AEM data that get compounded and contribute to the uncertainty of deriving a single model solution. When assessing and interpreting results, we need to address the question of determining which model is correct in reality. This section of the report uses probabilistic analyses to explore the characteristics of several acceptable models without being concerned about the details of any particular one.

The probabilistic approach of describing the inverse problem is to use a statistical framework and to attempt to describe or characterise the non-uniqueness of the solution by describing the solution in terms of the probability density function (pdf) in the model space. In many situations, we may have prior information to restrict the models to a small set of parameters, but even then different model parameter values either may be altered independently or may depend on other parameters to explain the observed data. The statistical approach enables one to estimate uncertainty bounds on the resulting model and the correlation between different model parameters. The advantages of the probabilistic approach are that it results in the marginal posterior probability density function of the model given the observed data and several measures of uncertainty in the model space can be obtained for a given parameterisation.

In this context, we have chosen the same line (highlighted in red in Figure 11) to illustrate one way of dealing with uncertainty. This example demonstrates how a Bayesian Markov chain Monte Carlo (MCMC) algorithm analysis can be used on this data. It used the Metropolis algorithm which is essentially a sampling algorithm in which a sample is first drawn from a trial (or proposal) distribution. This sample is then accepted or rejected using the Metropolis criterion. Its application is often restricted to relatively small problems because of the large number of forward model evaluations required for its convergence. A detailed description of the Trans-dimensional MCMC Inversion algorithm used here is beyond the scope of this report but can be found in Brodie and Sambridge (2012) and Sambridge (2014). In this report, we only provide a brief explanation of the results.

The employed Bayesian MCMC algorithm constructs an ensemble of thousands of 1D conductivity models at each AEM survey location. Each model is described by layer-conductivity and thickness values. It follows MCMC sampling rules and uses prior information consistent with the data (such as the likely thickness of conductive layer (conductance), and whether a 1D model was a reasonable starting point for the model structure). The number of layers used to describe each model is a free parameter, allowing for significant flexibility in the model parameterisation. By allowing the data to decide the necessary model complexity, errors associated with over- or under-fitting data and incorrect assumptions about model structure are avoided. It is a very computationally demanding procedure, which we have applied to a single line of the dataset as a trial.

With over 2000 measured sounding location data points along the line and 20,000 models per data point, Figure 19 is constructed from 40 million models derived by the MCMC. The method would work with only 10s of models for each point, but the uncertainty envelope would be very large, so this method is typically applied with 10s of thousands of models. On the top panel the mean and average misfit at each location are plotted as a profile in black and red respectively.

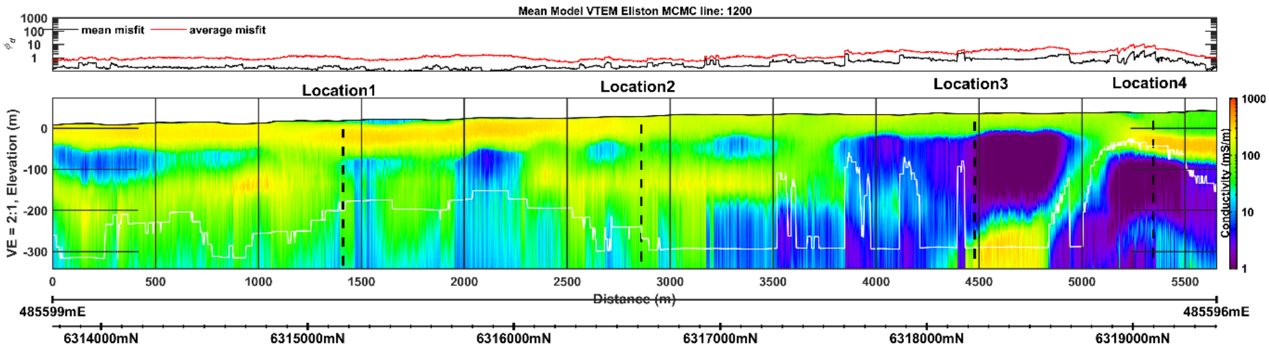

Figure 19 - Profile section of mean conductivity for VTEM Line 1200 (Mt Elliston), generated from the MCMC algorithm. Four locations have been selected to further inspect the models. The faint white line at the bottom of the section is the same estimated depth of investigation calculated from the smooth deterministic 30 layer inversion, plotted for reference.

The conductive wedge on the right-hand side of the section in Figure 19, a common feature in the previous inverted sections (e.g. Figure 9 and Figure 1613) is present but now portrayed as a thicker body. This shows the range of models that identify the wedge as an interface starting at ~ 50 m depths.

The presence of the less conductive features located between 3000 – 3500 m from the start of the line, which was described as potentially a fresh water lens in the interpretation of Figure 13, seems to be better mapped with its extent better defined in Figure 19.

To further inspect the MCMC, its results are compared with those derived from the deterministic inversions. The same four locations have been selected to look at the result with greater detail as shown in Figure 20. A range of probable distributions of conductivities as a function of depth is shown at each panel, for four different locations (Figure 20). The grey shading includes 90% of the credible models, which can be seen to spread out (asymmetrically) at depth due to a loss of resolution. The spread shows the wide range of models that fit the data. The dark blue curve is the lowest fitting curve from the MCMC, the mean model is shown in orange, the mode in green and the median in pink. The estimated depth of inversion at each location (determined from the 30-layer smooth inversion) is shown as a dotted brown line.

The cyan curves in each panel of Figure 20 correspond to the deterministic model obtained through the GA-LEI inversion (smooth 30-layers), which has been independently calculated. The plots show that that the deterministic inversions accurately recover the geo-electrical structure, are within the range of credible models, just as valid as the mean or mode models, and thus can be deemed to be representative of the whole suite of models at these locations. In the far-right panel of Figure 20, the conductivity values from ~200 m below the surface can be both resistive and conductive, which shows that it is therefore not resolvable.

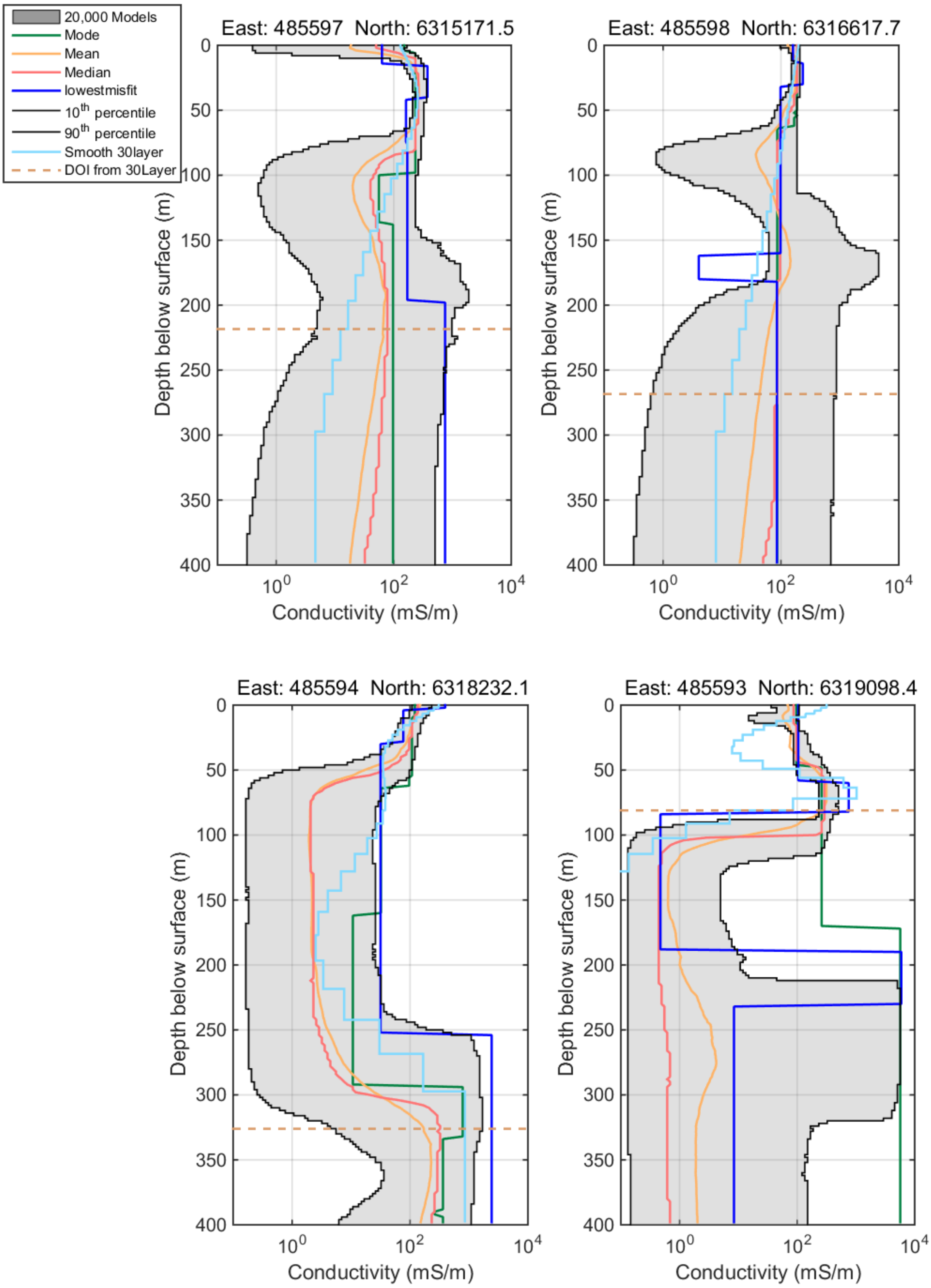

Figure 20 - Four locations along flight 1200 allows evaluation of results from 20 000 models which can all emulate and fit the measured data.

4 Results

System characteristics and geometry will determine the suitability of a given airborne EM system to map different targets. Approaches to the processing and inversion of derived data can also influence the modelled conductivity structure of the ground. Different inversion algorithms having the potential to generate different models of ground conductivity with the same data sets, so in order to minimise this effect we have inverted all available AEM data sets for the project area with a common inversion kernel (the GA-LEI). As a result of analysing the whole suite of datasets through inversion, the 17 legacy AEM datasets (shown in Figure 1) have been interpreted and hence inverted into maps that show the relative distribution of conductive material with depth (Figure 21 and Figure 22).

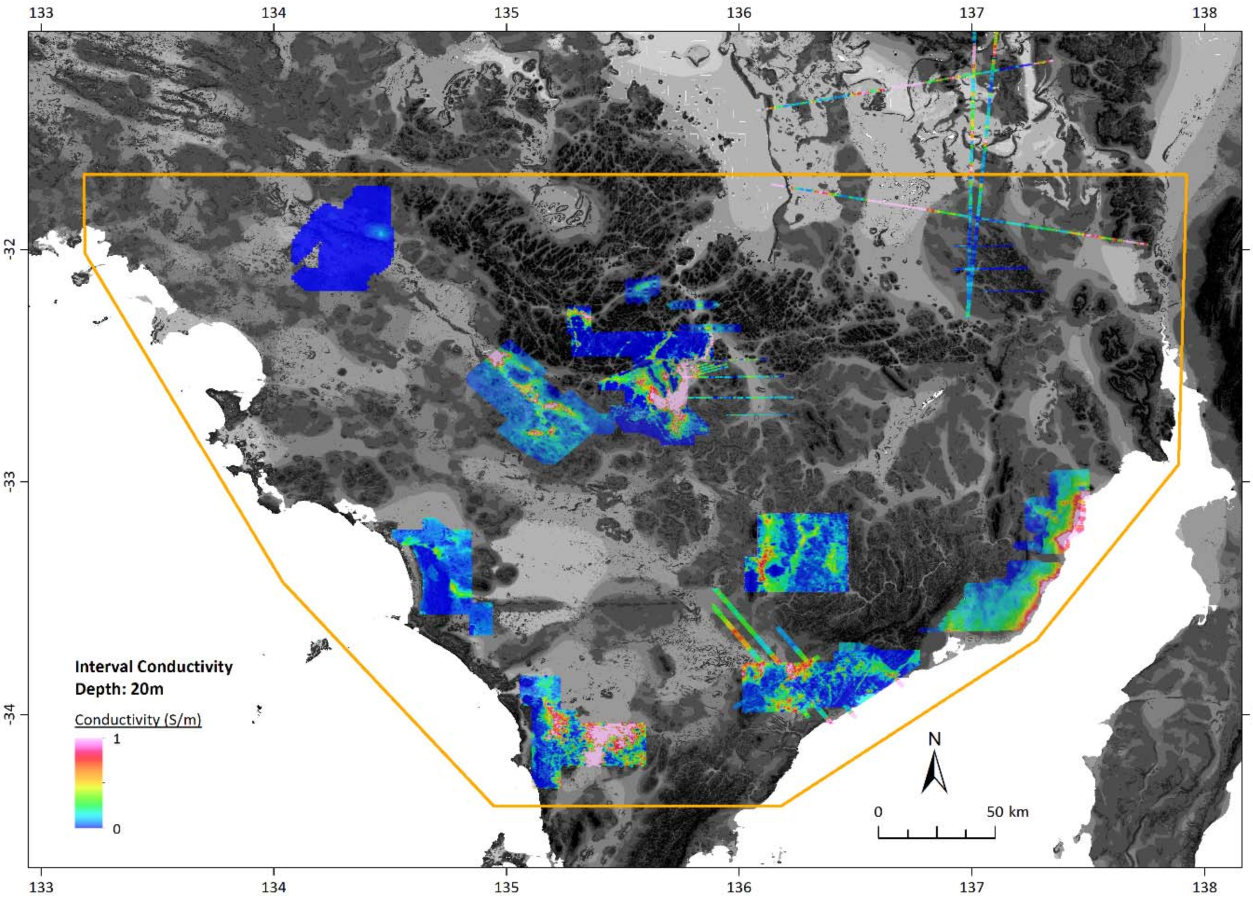

Figure 21 - Map of inverted conductivity derived form 17 datasets and 5 different airborne EM systems, at a depth slice range between ~20-25 m below the land surface.

From the two maps shown in Figure 21 and Figure 22, the more conductive materials (0.5 S/m and above) are mainly located in areas that are associated with salt water intrusion within close proximity to the coast, and in areas of flat lying topography where regolith materials such as transported sediments (including alluvial and colluvial materials composed of interbedded sands silts and clays with localised gravel units) have been mapped. Some of these conductors follow the contemporary drainage and are reflected as dendritic patterns which vary in their dimensions with depth. The mapping of these conductors with varying depths offers a great insight to the distributions of these features, their volumes and extensions. To accurately determine the materials which are responsible of these conductive responses, field-work including drilling would be an important aspect of future work in the area.

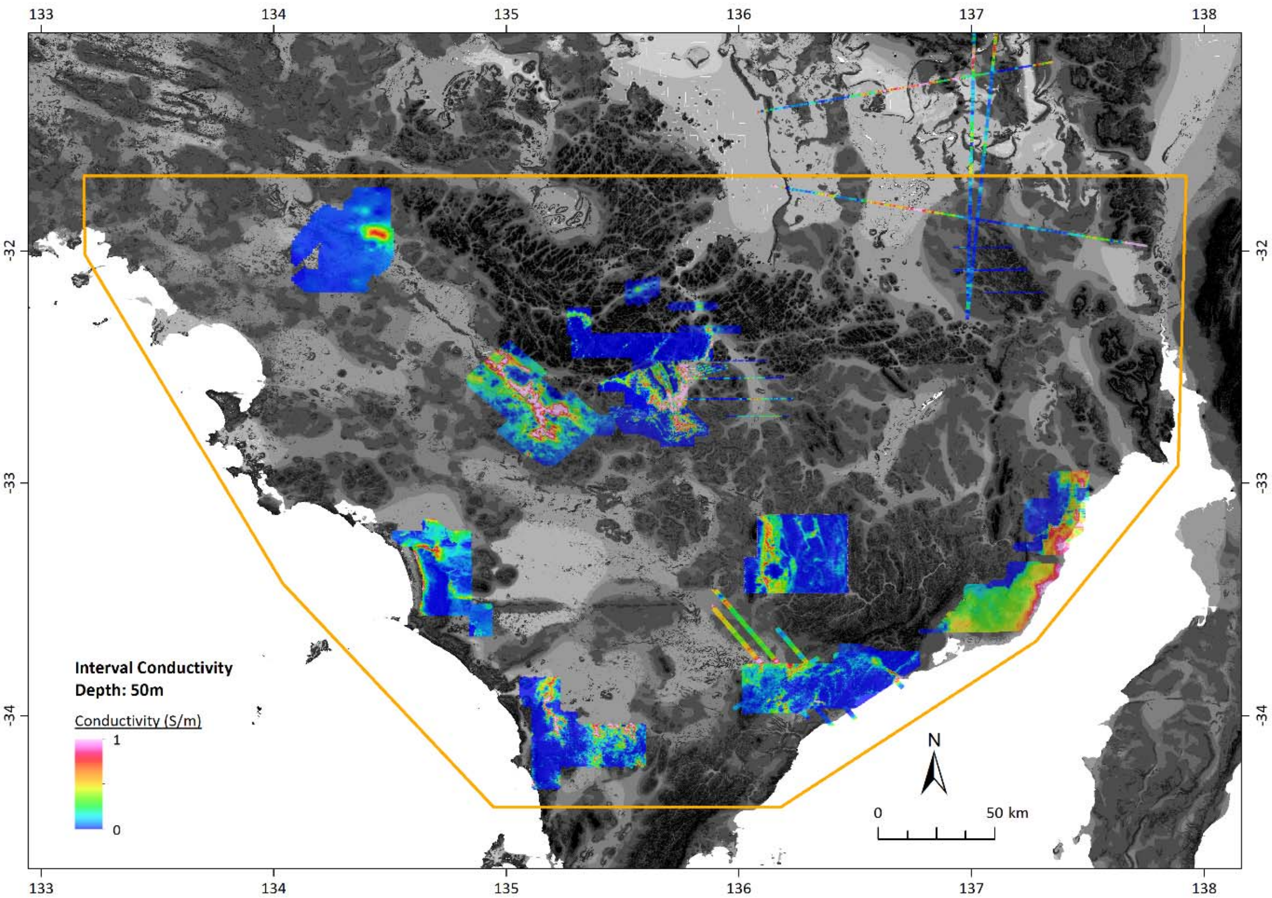

Figure 22 - Map of earth-forming materials'' conductivity distribution at a depth range of ~50-55 m below the land surface.

4.1 Data as a guide to model complexity

Layered-earth inversion of airborne electromagnetic (AEM) data is becoming ubiquitous with data collected during large regional surveys being able to be inverted in a matter of hours (e.g. Roach 2010). Despite the relative ease of application, it is often difficult to ascertain how robust the models are – particularly in the absence of other measured data and ground-truthing. Because of the nonlinearity of EM data, many models are able to theoretically fit the field data, especially when noise is accounted for. Typically, these questions are addressed by inverting data assuming different earth models, the appropriateness of these models can be assessed based on various error metrics. A more rigorous view of model robustness might be achieved through trans-dimensional Bayesian layered earth inversions (Brodie and Sambridge, 2012) at every station. However, such schemes are time consuming, and in any case, do not specifically address questions regarding layer continuity that are typically posed by AEM surveys. Thus, the application of a pragmatic (though non-rigorous) approach to assess model robustness would be very useful.

Earth response is modelled as a sum of exponentials (Stolz and Macnae, 1998). This is useful, firstly because it is more stable (mathematically) to model decaying signals as such sums (as opposed to power-law decays), and secondly, because data is not over-fitted, since the maximum number of terms in our sum is a function of the available data (a Tempest system with 15 gates allows sums of at most seven basis functions). Thus, sums composed of fewer terms represent simpler decays than sums composed of more terms.

The preferred model is the one for which the Bayesian information criterion (BIC) is minimised. The BIC is defined as:

$$BIC = n \ln \sigma_\varepsilon^2 + k \ \ln n$$

where n is the number of data points, k is the number of parameters and $\sigma_\varepsilon^2 = \sum_{i=1}^{n}(x_i - \bar{x}\,)^2$ is the error variance for n data points x_i and their mean $\bar{x}$.

This process is termed exponential basis-function decomposition (EBFD) and it is illustrated in Figure 23 for Station 632249 from Line 10600 in the Corunna Tempest survey. Different EBFDs are plotted in different colours along with their coefficient of fit (R^2). Generally fits to data are equally good when at least four basis functions are used. These different EBFD curves are the results of using different numbers of basis functions to make a range of different models.

Figure 23 shows results from fitting basis functions to multi-component AEM data that was acquired in this instance from the TEMPEST system. The upper part of Figure 23 shows fitting curves to the in-line component (x) of the data, while the lower part shows the fitting curve to the vertical component (y) of the data.

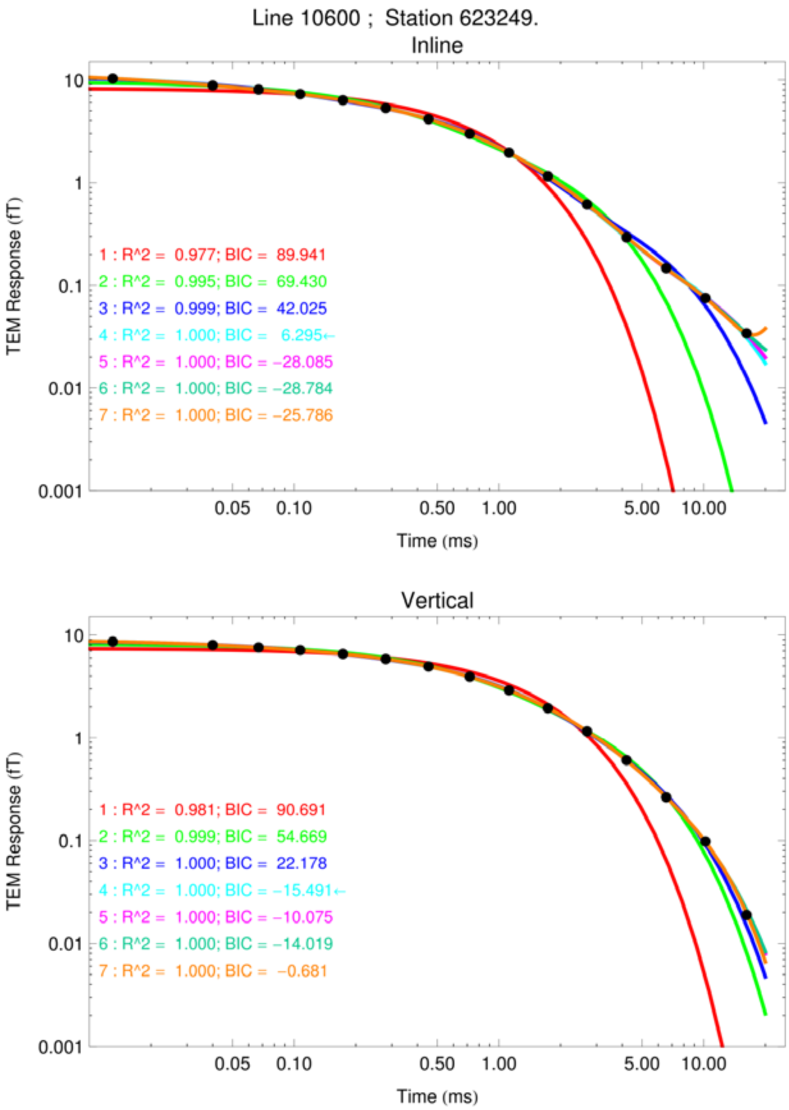

Figure 23 - Exponential basis-function decomposition (EBFD) for a range of different basis functions, applied to Tempest data from Corunna.

We applied these concepts to the Tempest data collected over Corunna. Figure 24 compares EBFD of inline and vertical component field data with multi-resolution valley-basement flatness (MrVBF) images (Gallant and Dowling, 2003). In both cases, there is some correspondence between maps of basis-function decomposition and the underlying image. For example, low flat areas generally have simple decompositions, while high areas with more curvature require more basis functions and might be considered as complex. Part of the survey that overflies Arno Bay also suggests simpler models as would be expected from conductive seawater. In this sense, EBFD permits some relationship to be drawn between the AEM data and the underlying geology.

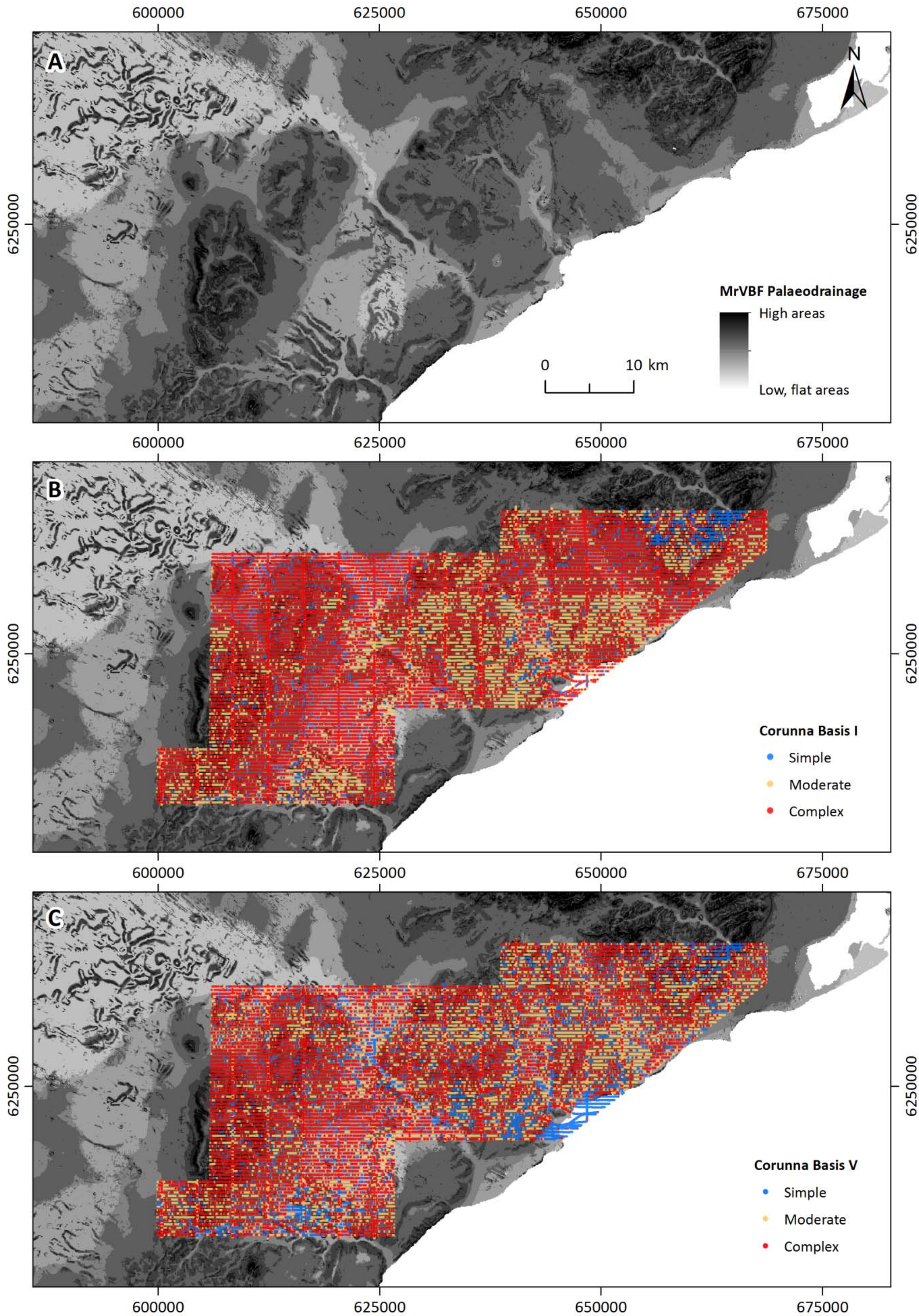

Figure 24 - Comparison between EBFD of inline and vertical component Tempest data and MrVBF (grey) images.

However, Figure 24 shows important differences between the underlying geo-data set and the decomposition. For example, intuitively, the hills north-east of the survey area should require more basis functions to fit data simply because of the geometric effects of the topography. EBFD in this area suggests that quite simple decays suffice.

The (at best) tenuous correlation between the EBFD and the underlying geology might be interpreted in terms of the nonlinear relationship between the AEM response and the earth. The AEM response is a complex function of the earth's conductivity, the transmitter, the receiver and the measurement system. Nonlinear inversion attempts to model the whole system, and is thus able to produce an earth model that is largely independent of the AEM system. Because it is a simple decomposition, EBFD considers the entire system, but is unable to untangle components. Thus, any conclusions one might draw regarding the correlation between the EBFD and the underlying earth range from tenuous (at best), and misleading (at worst).

For maximal benefits, curve-fitting must be based on an underlying physical model. Questions of model robustness must be addressed by examination of the model space. Examination of data space does not, in isolation provide clues to the underlying model. In retrospect, this too should have been obvious from an SVD (Golub and van Loan 1996) of the Jacobian.

$$\begin{aligned} J &= \frac{\partial d}{\partial p} \\ &= USV^t \end{aligned}$$

for data *d,* parameters *p* where *U* is the matrix of data space eigenvectors, *S* contains the singular values of *J*, and *V* is the matrix of model-space eigenvectors.

Perhaps the most solid conclusion that can be drawn from this exercise is that it is difficult to directly determine a relationship between measured data and the underlying regolith itself.

5 Discussion

In G-FLOWS Stage-2, considerable effort was given to compiling appropriate metadata on AEM system waveform, geometry, and bandwidth (gates), which all aid the inversion of the measured data. Accurate inversion and the derivation of sensible models of ground conductivity requires this information. A similar issue was encountered in G-FLOWS Stage-1 and this remains a significant impost on the common treatment and subsequent interpretation of the derived models of ground conductivity when dealing with legacy AEM data sets acquired for exploration.

The existing AEM data coverage across the northern Eyre Peninsula was scattered and had been acquired using a range of different systems. Whilst all data sets were inverted using a common inversion kernel, the derived models of subsurface conductivity were subject to limited constraint. Consequently their interpretation was predicated on this understanding, and all models were treated as being indicative of the true conductivity.

Validation of the data would have required considerable resource and ideally would have involved follow-up drilling and the use of ground and borehole geophysics (inductive conductivity logging and ground TEM). The scattered distribution of data across a large geographic region precluded this. The absence of open holes that could be logged (geophysically) also limited the value of such a ground exercise. Where available, publically available drill-hole and ground geophysical data was used (for example in the Cleve Hills area (Munday et al. 2015) to help interpret the physical association of subsurface conductivity with geology. However, much of the interpretation was subjective and qualitative.

Understanding the relationship between aquifer salinity and models of ground conductivity derived from the AEM data requires information on groundwater quality and about the aquifers themselves. The paucity of this information in the region hindered such analyses.

From a geophysical inversion perspective, the approach to constraining inversion results through the development of calibration procedures has been progressed in G-FLOWS Stage-2. A method employing selective sampling of ground surface TDEM data was demonstrated to allow inverted products from overlapping AEM data sets from different systems to be standardised and merged. Borehole inductive conductivity logs also have value in this regard, although consideration of the footprints of the systems involved needs to be considered. The use of constraints from flying over sea water was also demonstrated to have application in the “calibration” of data from an uncalibrated system. The result was the generation of sensible (realistic) models of ground conductivity.

Deterministic inversion methods (e.g. GA-LEI and AarhusInv) have been demonstrated to work effectively with data from a range of systems and vintages, generating robust models of subsurface conductivity structure rapidly, particularly where system information is available. These approaches will continue to have value in the incorporation of exploration data sets for groundwater and aquifer characterisation, but their real value will only be realised where the data are used in conjunction with conventional hydrogeological information.

Newer stochastic EM inversion approaches are showing considerable promise, particularly in helping determine the conductivity structure and providing uncertainty estimates relating to aquifer bounds and to attributed values of conductivity. The potential remains to assess these methods for inverting directly for lithology (aquifer-type) and lithological bounds, providing uncertainty associated with these. These should be tested with geophysical data sets in data poor areas when groundwater assessments might be undertaken.

6 Summary

When interpreting and modelling airborne EM data, errors are introduced in the models if the system specifications are inexact (e.g. insufficient specifications, software limitations), and this is particularly problematic when dealing with legacy data. Accounting for accurate system characterisation enables the derivation of a quantitative analysis of conductivity-depth models. These models, when analysed in the context of landscape morphology and their geographical locations, can contribute to the development of the conceptual hydrogeological models. It is important that this is undertaken in conjunction with other lines of evidence, such as by acquiring ground-based geophysical data at representative locations and comparing results, comparing water well data with conductivity patterns, and also by incorporating existing geological and hydrological information into the interpretation of the airborne geological data.

Standard deterministic inversion looks for a single 'best' model through an iterative processes using an optimization function. Overall, this work shows that deterministic inversions can accurately recover the broad type of geo-electrical structures, which are sought after when looking at regional hydrological features. Unfortunately, this approach does not provide comprehensive uncertainty quantification.

By using an MCMC algorithm on one of the AEM datasets of this work, thousands of varying plausible simulations have been sampled, which allowed changes in the number of layers, thicknesses, depths and conductivity values. The results show that there is a large range of models that are consistent with the measured data. The high density number of models allows a formal statistical analysis, which can quantitatively evaluate the degree of uncertainty of each of the proposed models at every individual location thus enabling us to query models and assumptions. The MCMC analysis has mostly shown that properly modelled deterministic inversions can accurately recover and represent the geo-electrical structure of the undelaying geology, albeit with a single representation. The deterministic model generally within the set of possible solutions identified by MCMC, but the uncertainty band for MCMC is often very wide, and the deterministic solution of often quite different from the mean.

Modelling the whole suite of datasets has enabled us to transform legacy AEM data into maps and cross-sections that show the distribution of conductive materials with depth. Results show that conductive materials are mapped in areas associated with salt water intrusion and also where regolith materials such as transported sediments (alluvial and colluvial materials composed of interbedded sands silts and clays with localised gravel units) are abundant. Mapping conductors at varying depths provides an insight into distributions, volumes and extensions to potential aquifers and other sediment-filled features.

A drilling program is needed to identify the materials that are responsible for the main conductive responses. It is worth noting that when interpreting EM results one should consider the fact that model-layers often represent several lithological layers, particularly in the case of a sedimentary sequence comprising several small interbedded layers. We conclude that stratigraphic interpretation of conductivity is only possible in cases of a sufficient lithological change that can be correlated with a strong change in conductivity.

7 Recommendations

- Geological Survey of South Australia develop and maintain a directory of metadata relating to AEM systems and related surveys that details: date of acquisition, AEM system used, waveform employed, time gates used, and nominal system geometry.
- Derived models of subsurface conductivity from the inversion of AEM data sets should, in the absence of supporting drill-hole and ground data, be treated as providing a qualitative indication of groundwater quality and aquifer character. Where more detailed groundwater resource assessments are being undertaken in areas where AEM data are available, then work should be undertaken to validate derived conductivity models to inform groundwater model development as appropriate.
- Validation using results from targeted drilling be undertaken, including aquifer characterisation (petrophysical and hydraulic properties), borehole logging, aquifer testing, water sampling and analyses (tracers, Isotopes, and chemistry). A deficiency of both G-FLOWS Stage-1 and Stage-2 was the lack of available on-ground data to undertake detailed validation work, which can underpin the hydrogeological framework models that have been developed. Future projects should have a significant resource devoted to this.

8 Conclusions

The project has shown that AEM geophysical data can be inverted using MCMC analysis. The project has demonstrated the value of taking exploration geophysical datasets and applying them to enhance our understanding of the hydrogeology of the remote parts of South Australia.

The main conclusions from this report are:

- This project used a consistent approach to the processing and geophysical interpretation (inversion) of AEM datasets acquired for an exploration purpose in a hydrogeological context. This task is difficult as there are differences between the various acquisition systems that need to be accounted for in order to provide comparable models in a regional setting.
- Robust deterministic inversion methods are effective in providing valid representations of the conductivity structure of the ground. Full inversion of legacy AEM data sets indicates that more complex information on the ground conductivity structure, can be obtained after comparing them with results derived from direct transforms or apparent conductivity calculations. Their effectiveness is largely attributable to a reasonable understanding of the landscape and its variability in the subsurface. However, standard deterministic approaches of data interpretation do not take into account the uncertainties in defining layer boundaries and conductivities. A more rigorous view of model robustness might be attained through trans-dimensional Bayesian layered earth inversions.
- To investigate this further, the project undertook a Markov chain Monte Carlo Inversion (MCMC) analysis for a dataset in the Eyre Peninsula. This has indicated that the geo-electric structure of the ground can be represented by a range of models, and layer boundaries can be defined with associated uncertainties. This work also suggested that properly constrained deterministic approaches can provide a reasonable model of the subsurface conductivity structure. Further studies should be carried out to investigate how these uncertainties can be incorporated into hydrogeological modelling for groundwater resource assessment.

9 References

Boulding JR (1993) Use of Airborne, Surface and Borehole Geophysical Techniques at Contaminated Sites: A Reference Guide. EPA/625/R-92/007. Office of Science Planning and Regulatory Evaluation, U.S. EPA, Cincinnati, OH, USA.

Boyd, G.W. (2004) HoistEM – a new airborne electromagnetic system. PACRIM 2004, Adelaide, South Australia, 19-22 September 2004, 211-218.

Brodie R, and Sambridge M (2012) Transdimensional Monte Carlo Inversion of AEM Data. ASEG Extended Abstracts 2012(1) 1-4.

Brodie R, Green A, and Munday T (2004) Constrained inversion of helicopter AEM data for mapping the Blanchetown Clay. Extended Abstract, ASEG 17th Geophysical conference and exhibition, Sydney. Available from: http://www.publish.csiro.au/?act=view_file&file_id=ASEG2004ab013.pdf

Christiansen AV, Auken E, and Viezzoli A (2011) Quantification of modeling errors in airborne TEM caused by inaccurate system description. Geophysics 76(1), F43–F52. http://dx.doi.org/10.1190/1.3511354

Davis AC, and Macnae J (2008) Quantifying AEM system characteristics using a ground loop. Geophysics 73(4), F179-F188. doi: 10.1190/1.2943189

Emerson DW, and Yang YP (1997) Effects of water salinity and saturation on the electrical resistivity of clays. Preview 68, 19-24.

Everett ME (2013) Near surface applied geophysics. Cambridge University Press.

Fitterman DV, and Deszcz-Pan M (2001) Saltwater Intrusion in Everglades National Park, Florida Measured by Airborne Electromagnetic Surveys. In proceeding of First International Conference on Saltwater Intrusion and Coastal Aquifers Monitoring, Modeling, and Management. Essaouira, Morocco, April 23—25, 2001. Available from: http://www.olemiss.edu/sciencenet/saltnet/swica1/Fitterman-Deszcz-Pan-paper.pdf

Gallant JC, and Dowling TI (2003) A multiresolution index of valley bottom flatness for mapping depositional areas. Water Resources Research 39 (12), 1347, doi:10.1029/2002WR001426

Gilfedder M, Munday T (2013) Facilitating Long-term Outback Water Solutions (G-FLOWS Stage-1) Final Report. Goyder Institute for Water Research Technical Report Series No. 13/13.

Golub GH, and Van Loan CF (1996) Matrix computations. Third edition. Johns Hopkins University Press, Baltimore, MD, USA, 374-426.

Ley-Cooper AY, Macnae J, and Viezzoli A (2010) Breaks in lithology: Interpretation problems when handling 2D structures with a 1D approximation. Geophysics 75(4), WA179-WA188. doi: 10.1190/1.3483101

Ley-Cooper AY, Munday TJ (2013) Groundwater Assessment and Aquifer Characterization in the Musgrave Province, South Australia: Interpretation and Assessment of SPECTREM Airborne Electromagnetic Data. Goyder Institute for Water Research Technical Report Series No. 13/7.

Loke MH (2000) Electrical imaging surveys for environmental and engineering studies. A practical guide to 2-D and 3-D surveys. 61 pp. Viewed Dec 3 2015, available from http://moho.ess.ucla.edu/~pdavis/ESS135_2013/LITERATURE/%20LokeDCREsistivity.pdf

Macnae J, King A, Stolz N, Osmakoff A, and Blaha A (1998) Fast AEM data processing and inversion: Exploration Geophysics 29, 163–169.

McNeill JD (1980) Electromagnetic terrain conductivity measurement and low induction numbers. Technical Note TN-6, Geonics Limited. http://www.geonics.com/pdfs/technicalnotes/tn6.pdf

McNeill JD (1990) Influence of Galvanic Currents on Electromagnetic Surveys. Symposium on the Application of Geophysics to Engineering and Environmental Problems 1990, 223-227. doi:10.4133/1.2921880

Munday T, Mann S, Ley Cooper Y, Ferris G, and Keates K (2015) Graphite in the Eyre Peninsula of South Australia – Geophysics over “flaky” ground. KEGS Symposium 2015 Exploration for Strategic minerals, Toronto, Canada, 28/2/2015, 45–49.

Paine JG, and Collins EW (2003). Applying airborne electromagnetic induction in groundwater salinization and resource studies, West Texas. In Proceedings of 16th EEGS Symposium on the Application of Geophysics to Engineering and Environmental Problems, Environmental and Engineering Geophysical Society: 722-738.

Palacky GJ (1983) Tutorial: research, applications, and publications in electrical and electromagnetic methods. Geophysical Prospecting 31(6), 861 - 872. doi:10.1111/j.1365-2478.1983.tb01094.x

Palacky GJ (1988) Resistivity characteristics of geologic targets, in Investigations in Geophysics vol. 3: Electromagnetic methods in applied geophysics-theory, vol. 1, edited by MN Nabighian, Soc. Expl. Geophys., 53–129.

Peters WS (2001) Ground electromagnetics: the basics and recent developments. Recent Developments and Future Directions in Geophysics. AIG Bulletin 33, 15-32.

Rhoades JD, Raats PAC, and Prather RJ (1976) Effects of liquid-phase electrical conductivity, water content, and surface conductivity on bulk soil electrical conductivity. Soil Science Society of America Journal 40(5), 651-655. doi:10.2136/sssaj1976.03615995004000050017x

Risby L, and Harrington G (2014) Non-prescribed groundwater resources assessment - Eyre Peninsula Natural Resources Management Region. Phase 2 - Hydrogeochemistry. DEWNR Technical Report 2014/10, Department of Environment, Water and Natural Resources, Adelaide. Available from: https://www.waterconnect.sa.gov.au/Content/Publications/DEWNR/DEWNR_TR_2014-10.pdf

Roach IC (Ed.) (2010). Geological and energy implications of the Paterson Province airborne electromagnetic (AEM) survey, Western Australia. Geoscience Australia Record 2010/12, 318 pp.

Sambridge M (2014) A Parallel Tempering algorithm for probabilistic sampling and multimodal optimization. Geophysical Journal International 196, 357–374. doi: 10.1093/gji/ggt342

Schamper C, Auken E, and Sørensen K (2014) Coil response inversion for very early time modelling of helicopter-borne time-domain electromagnetic data and mapping of near-surface geological layers. Geophysical Prospecting 62(3). 658–674. doi: 10.1111/1365-2478.12104

Siemon B, Christiansen AV, and Auken E (2009) A review of helicopter-borne electromagnetic methods for groundwater exploration. Near Surface Geophysics 7(5–6), 629–646

Stolz EM, and Macnae J (1998) Evaluating EM waveforms by singular-value decomposition of exponential basis functions. Geophysics 63(1), 64–74. doi: 10.1190/1.1444328

Taylor AR, Pichler MM, Olifent V, Thompson J, Bestland E, Davies PJ, Lamontagne S, Suckow A, Robinson N, Love A, and Munday T (2015) Groundwater Flow Systems of North-eastern Eyre Peninsula (G-FLOWS Stage-2): Hydrogeology, geophysics and environmental tracers. Technical Report Series No. 15/37, Goyder Institute for Water Research, Adelaide.

Viezzoli A, Jørgensen F, Sørensen C (2013) Flawed Processing of Airborne EM Data Affecting Hydrogeological Interpretation. Groundwater 51(2), 191-202. doi:10.1111/j.1745-6584.2012.00958.x

Vrbancich V (2011) Airborne electromagnetic bathymetry investigations in Port Lincoln, South Australia – comparison with an equivalent floating transient electromagnetic system. Exploration Geophysics 42(3), 167–175.

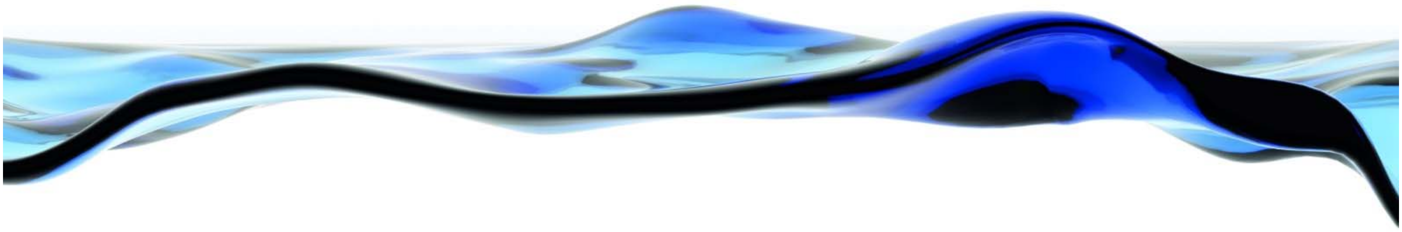

The Goyder Institute for Water Research is a partnership between the South Australian Government through the Department of Environment, Water and Natural Resources, CSIRO, Flinders University, the University of Adelaide and the University of South Australia.